



INDC(NDS)-0731
Distr. AC/AD/G/IN/J/RD/SC/ST

INDC International Nuclear Data Committee

Summary Report of the Third Research Coordination Meeting on Testing and Improving the International Reactor Dosimetry and Fusion File (IRDFF)

IAEA Headquarters, Vienna, Austria

20-24 March 2017

Prepared by

L.R. Greenwood, Pacific Northwest National Laboratory, Richland, WA, USA

M. Kostal, Nuclear Physics Institute, Rez, Czech Republic

S.P. Simakov, Institute for Neutron Physics and Reactor Technology - Karlsruhe Institute for
Technology (KIT), Karlsruhe, Germany

A. Trkov, Nuclear Data Section, IAEA, Vienna, Austria

August 2017

IAEA Nuclear Data Section
Vienna International Centre, P.O. Box 100, 1400 Vienna, Austria

Selected INDC documents may be downloaded in electronic form from

<http://www-nds.iaea.org/publications>

or sent as an e-mail attachment.

Requests for hardcopy or e-mail transmittal should be directed to

NDS.Contact-Point@iaea.org

or to:

Nuclear Data Section

International Atomic Energy Agency

Vienna International Centre

PO Box 100

1400 Vienna

Austria

Printed by the IAEA in Austria

August 2017

Summary Report of the Third Research Coordination Meeting on
**Testing and Improving the International Reactor Dosimetry and
Fusion File (IRDF)**

IAEA Headquarters, Vienna, Austria

20-24 March 2017

Prepared by

L.R. Greenwood, Pacific Northwest National Laboratory, Richland, WA, USA

M. Kostal, Nuclear Physics Institute, Rez, Czech Republic

S.P. Simakov, Institute for Neutron Physics and Reactor Technology - Karlsruhe Institute for
Technology (KIT), Karlsruhe, Germany

A. Trkov, Nuclear Data Section, IAEA, Vienna, Austria

ABSTRACT

The Third Research Coordination Meeting on Testing and Improving the International Reactor Dosimetry and Fusion File (IRDF) was held at the IAEA Headquarters in Vienna on 20-24 March 2017. The purpose of the Meeting was to review the developments since the previous Meeting, reflected in the contributions by the participants. A number of reactions were included for neutron dosimetry up to 100 MeV and new integral experiments were performed for the validation of the library. It was decided to include all the corrections and extensions to the IRDF library in a new release named IRDF-2.0.

August 2017

Contents

| | |
|---|-----------|
| 1. Present Status of the IRDFF Database | 7 |
| 1.1. Some outcomes from the IAEA CRP F41031 “Testing and Improving the International Reactor Dosimetry and Fusion File (IRDFF)”, S. Simakov | 7 |
| 2. Measurements of Nuclear Data | 7 |
| 2.1. The use of integral experiments for nuclear data benchmarking, M. Kostal | 7 |
| 2.2. Experimental validation of IRDFF cross-sections in quasi-monoenergetic neutron fluxes in 20-35 MeV energy range, E. Šimečková..... | 7 |
| 2.3. Activation cross section measurements for Bi and Co by 80 and 140 MeV p-Li quasi-monoenergetic neutrons, H. Yashima..... | 8 |
| 2.4. Cross-section measurements for neutron-induced reactions in Co, Au, Bi and Tm at neutron energy of 90 and 140 MeV, N.B. (Zina) Ndlovu | 8 |
| 2.5. Results of integral cross section measurements and nuclear data performed at CEA reactor facilities, C. Destouches | 8 |
| 3. Nuclear Data Evaluation..... | 9 |
| 3.1. Re-evaluation of the $^{23}\text{Na}(n,\gamma)^{24}\text{Na}$, $^{23}\text{Na}(n,2n)^{22}\text{Na}$ and $^{27}\text{Al}(n,2n)^{26}\text{Al}$ reaction excitation functions from threshold to 60 MeV, K. Zolotarev | 9 |
| 3.2. Analysis and updating of the nuclear decay data evaluations to improve the IRDFF Decay sub-library, V. Chechev | 9 |
| 4. Nuclear Data Verification and Validation | 10 |
| 4.1. Advanced UQ approaches to the validation of dosimetry cross sections in reactor benchmark fields: Input to 3 rd RCM, P. Griffin | 10 |
| 4.2. Benchmarking of IRDFF against 14 MeV neutronics experiments at ENEA Frascati, M. Angelone | 11 |
| 4.3. Final results of IRDFF benchmark experiments at JAEA/FNS, C. Konno | 12 |
| 4.4. Improvements to STAYSL PNNL spectral adjustment with IRDFF, L.R. Greenwood | 12 |
| 4.5. Analysis of ASPIS-IRON88 benchmark and TRIGA measurements for IRDFF validation and proposals for the REAL-201X adjustment exercise, I. Kodeli | 13 |
| 5. Actions | 13 |
| 5.1. Status of Actions from the 2nd RCM for the Improvement of IRDFF | 13 |
| 5.2. New Actions Emerging from the Discussions during the 3rd RCM..... | 16 |
| 6. Outline of the Final CRP Report | 18 |
| 7. Participants’ Summaries..... | 19 |
| 7.1. Manage and technical contribution of NDS to CRP on the IRDFF testing, improving and validation, S. Simakov | 19 |
| 7.2. Experimental Validation of IRDFF Cross-Sections in Quasi-MonoEnergetic Neutron Fluxes in 20-35 MeV Energy Range, M. Majerle, P. Bém, J. Novák, E. Šimečková, M. Štefánik | 24 |
| 7.3. Analyzing and updating nuclear decay data evaluations to improve the IRDFF Decay sub-library, V. Chechev | 26 |
| 7.4. Advanced UQ Approaches to the Validation of Dosimetry Cross Sections in Reactor Benchmark Fields: Input to 3 rd RCM, P. Griffin..... | 28 |
| 7.5. Benchmarking of IRDFF Against 14 MeV Neutron Experiments, M. Angelone | 36 |
| 7.6. Final results of IRDFF benchmark test at JAEA/FNS, M. Ohta ¹ , S. Sato ¹ , S. Kwon ¹ , K. Ochiai ¹ , C. Konno ² | 38 |
| 7.7. Improvements to STAYSL PNNL Spectral Adjustment with IRDFF, L.R. Greenwood, C.D. Johnson..... | 43 |
| APPENDIX 1 - Preliminary Agenda..... | 49 |
| APPENDIX 2 - List of Participants..... | 51 |

1. Present Status of the IRDFF Database

Highlights from the presentations by participants and the discussions are summarized below.

1.1. Some outcomes from the IAEA CRP F41031 “Testing and Improving the International Reactor Dosimetry and Fusion File (IRDFF)”, S. Simakov

Institute for Neutron Physics and Reactor Technology -Karlsruhe Institute of Technology (KIT), Eggenstein-Leopoldshafen, Germany

Taking into consideration the latest evaluations presented at this Meeting, there are now 81 total reactions in the IRDFF library, 6 of which were new additions and 7 of which were updates that took place during the CRP period.

Additionally, seven high-threshold $^{209}\text{Bi}(n,xn)^{210-x}\text{Bi}$ reactions are included, where $x = 4 - 10$, which support neutron dosimetry up to 100 MeV. These reactions were evaluated by V. Pronayev using the least-squared method (GMA code) and were based on experimental cross sections measured by the CRP participants and other experimentalists. The participants of RCM-3 recommend the inclusion of these evaluations into IRDFF.

2. Measurements of Nuclear Data

2.1. The use of integral experiments for nuclear data benchmarking, M. Kostal

Nuclear Physics Institute, Rez, Czech Republic

The experimental campaign on LR-0 focused on measurements of spectral-averaged cross sections in the LR-0 neutron field and also in the $^{252}\text{Cf}(s.f.)$ field (at CV Rez the ^{252}Cf source strength is $1\text{E}9$ n/s). It was demonstrated that the LR-0 spectrum is indistinguishable from the ^{235}U PFNS in the energy region above 6 MeV. In LR-0, the (n,2n) reactions were measured for ^{75}As , ^{23}Na , ^{89}Y , and ^{90}Zr .

In $^{252}\text{Cf}(s.f.)$, there were measurements of the $^{54}\text{Fe}(n,p)$, $^{54}\text{Fe}(n,\alpha)$, $^{23}\text{Na}(n,2n)$, $^{27}\text{Al}(n,p)$, $^{27}\text{Al}(n,\alpha)$, $^{18}\text{F}(n,2n)$, $^{90}\text{Zr}(n,2n)$ and $^{89}\text{Y}(n,2n)$ reaction rates as well as reaction rates of (n, γ) for ^{94}Zr and ^{96}Zr which can be used for cross section validation.

There are plans to continue measurements of other reactions including $^{27}\text{Al}(n,\alpha)$, $^{127}\text{I}(n,2n)$, $^{19}\text{F}(n,2n)$ and $^{55}\text{Mn}(n,2n)$ at the LR-0 facility. Experiments are in progress with the $^{252}\text{Cf}(s.f.)$ source to measure the (n,2n) SPA cross sections on Tm, Au, Nb, ^{56}Fe , ^{130}Te , Co, Y and Mn.

2.2. Experimental validation of IRDFF cross-sections in quasi-monoenergetic neutron fluxes in 20-35 MeV energy range, E. Šimečková

Nuclear Physics Institute (NPI), Rez, Czech Republic

The scope of this work was the validation of the cross-sections for neutron dosimetry reactions on ^{54}Fe , ^{59}Co , ^{169}Tm , ^{197}Au and ^{209}Bi in the energy range 20-35 MeV. The samples of these isotopes were irradiated using the NPI quasi-monoenergetic neutron source based on the $p+^7\text{Li}$ reaction and the activated products were measured by gamma-spectrometry.

Seven proton energies were used: 20, 22.5, 25, 27.5, 30, 32.5 and 35 MeV. The neutron spectrum from the $p+^7\text{Li}$ reaction consists of the monoenergetic peak and the lower energy continuum. The extraction procedure based on the SAND-II unfolding code was used to obtain the cross-sections from the measured activities. The neutron spectrum was accurately determined using the Time-of-Flight measurements and the absolute number of neutrons in the peak was determined from the ^7Be activity of the lithium target. The uncertainties of the final results were evaluated by sensitivity analysis and were determined to be within 10% for most extracted cross-sections.

Some inconsistencies were observed when a $^{\text{nat}}\text{Li}$ target was used instead of a ^7Li -enriched target. This is worth further investigation. We also plan to continue high energy cross section measurements for W, Ta and Zr elements.

2.3. Activation cross section measurements for Bi and Co by 80 and 140 MeV p-Li quasi-monoenergetic neutrons, H. Yashima

Kyoto University-Research Reactor Institute, Osaka, Japan

Neutron activation experiments for Bi and Co were performed using 80 and 140 MeV p-Li quasi-monoenergetic neutron beams. The energy spectra of this neutron field are not purely monoenergetic, with both a high energy peak coming from the ${}^7\text{Li}(p,n)$ reaction, and a low energy tail resulting from the consequent break-up reaction. The contributions from low energy neutrons were corrected by the ratio of reaction rates, using the peak neutron-to-total reaction rate measured in the experimental data by Kim *et al.* and the JENDL-4.0/HE data file. There are still some problems with the subtraction of low energy neutrons.

The neutron activation cross sections of the ${}^{209}\text{Bi}(n,xn)^{203,204,205,206}$ and ${}^{59}\text{Co}(n,xn)^{56,57,58}$ reactions were obtained for the 80 and 140 MeV p-Li quasi-monoenergetic neutron beams, whose peak neutron energies are 76 and 134 MeV, respectively. These results generally agree with results by Kim *et al.*, except for the ${}^{59}\text{Co}(n,4n)^{56}\text{Co}$ reaction.

Comments: Comparisons should be made with other measured data available in EXFOR and with the evaluation of V. Pronyaev for ${}^{209}\text{Bi}(n,xn)$ reactions.

2.4. Cross-section measurements for neutron-induced reactions in Co, Au, Bi and Tm at neutron energy of 90 and 140 MeV, N.B. (Zina) Ndlovu

iThemba Laboratory for Accelerator-based Sc., Somerset West, South Africa

Neutron activation experiments on various targets (Co, Au, Bi and Tm) using 90 and 140 MeV quasi-monoenergetic neutron beams were performed at iThemba LABS. Two identical target stacks (front to back arrangement, Al-Cu-Co-Tm-Bi-Au-Al) were irradiated simultaneously for each measurement, one in the 0° and the other in the 16° beam lines. Both the Al and Cu targets are used as neutron fluence monitors in the stack. Preliminary results for gamma-ray spectra were obtained for the irradiated targets, ${}^{59}\text{Co}$, ${}^{169}\text{Tm}$, ${}^{197}\text{Au}$ and ${}^{209}\text{Bi}$ (with additional gamma-ray spectra for ${}^{\text{nat}}\text{Al}$ and ${}^{\text{nat}}\text{Cu}$ (monitor foils)). Neutron fluence data are obtained by subtracting the data measured at 16° from the data measured at 0° , and this has been inconsistent with expectations. Further analysis of neutron beam detectors and monitors is required to finalize cross section data.

2.5. Results of integral cross section measurements and nuclear data performed at CEA reactor facilities, C. Destouches

CEA – Centre d'études nucléaires de Cadarache, St. Paul Lez Durance, France

An overview of the integral cross section measurements performed at the CEA reactor facilities from the point of view of applicability to IRDFF validation (data presented are drawn from previously published papers) was presented. First, experimental measurements of capture cross sections performed at the MINERVE facility during the MAESTRO program were presented: ${}^{115}\text{In}(n,\gamma)$, ${}^{59}\text{Co}(n,\gamma)$, ${}^{55}\text{Mn}(n,\gamma)$ and ${}^{109}\text{Ag}(n,\gamma)$. In addition, the emission intensities and decay period evaluation for ${}^{116\text{m}}\text{In}$ are presented. Experimental data measured at the EOLE facility are also presented in terms of C/E for the ${}^{51}\text{V}(n,\alpha)$, ${}^{27}\text{Al}(n,\alpha)$, ${}^{46}\text{Ti}(n,p)$, ${}^{54}\text{Fe}(n,p)$, ${}^{58}\text{Ni}(n,p)$, ${}^{115}\text{In}(n,n')$, ${}^{103}\text{Rh}(n,n')$, ${}^{117}\text{Sn}(n,n')$, ${}^{59}\text{Co}(n,\gamma)$ and ${}^{197}\text{Au}(n,\gamma)$ reactions. The status of experimental data measured at MASURCA and CALIBAN facilities was presented. Work performed at CEA during the CRP on the ${}^{92,94}\text{Zr}(n,\gamma)$ and ${}^{117}\text{Sn}(n,n')$ ${}^{117\text{m}}\text{Sn}$ reactions as epithermal dosimeters was then summarized. Finally, after the presentation of ${}^{103}\text{Rh}(n,n')$ ${}^{103\text{m}}\text{Rh}$ and ${}^{93}\text{Nb}(n,n')$ ${}^{93\text{m}}\text{Nb}$ nuclear data studies that were conducted at the CEA over the last two years, the CALMAR adjustment code publication status was presented. The presentation concluded by listing the remainder of the actions that have been achieved in order to promote cross section measurements with ${}^{252}\text{Cf}$ sources.

Comments: It was recommended that the CEA current reaction rates (using the recommended template for reporting activation measurements) and neutron spectra (using the 640 energy groups), in addition to C/E values, should be made available for the validation of IRDFF.

3. Nuclear Data Evaluation

3.1. Re-evaluation of the $^{23}\text{Na}(n,\gamma)^{24}\text{Na}$, $^{23}\text{Na}(n,2n)^{22}\text{Na}$ and $^{27}\text{Al}(n,2n)^{26}\text{Al}$ reaction excitation functions from threshold to 60 MeV, K. Zolotarev

Institute of Physics and Power Engineering (IPPE), Obninsk, Russian Federation

At the RCM-3, two updated evaluations for the $^{23}\text{Na}(n,\gamma)^{24}\text{Na}$ and $^{23}\text{Na}(n,2n)^{22}\text{Na}$ reactions, plus two new evaluations for the $^{27}\text{Al}(n,2n)^{26m}\text{Al}$ and $^{27}\text{Al}(n,2n)^{26g}\text{Al}$ reactions were presented by K. Zolotarev.

The new re-evaluation of the $^{23}\text{Na}(n,\gamma)^{24}\text{Na}$ reaction cross section and the uncertainties have been carried out in the energy region 1.0E-05 eV to 20 MeV. From 1.0E-05 eV to 459.3 keV, it is represented via the Reich-Moore (RM) resonance parameters. The upper boundary of the resolved resonance region is limited by the threshold of inelastic scattering. The obtained resonance parameters permit calculation of the $^{23}\text{Na}(n,\text{total})$, $^{23}\text{Na}(n,\text{elastic})$ and $^{23}\text{Na}(n,\gamma)^{24}\text{Na}$ excitation functions in the neutron energy range 1.0E-05 eV – 459.3 keV without the need for additional background cross sections in tabular form. This was not the case for IRDF-2002, where the evaluated $^{23}\text{Na}(n,\gamma)^{24}\text{Na}$ reaction cross section (taken from ENDF/B-VI) had a significant background in the resolved resonance region.

The $^{23}\text{Na}(n,2n)^{22}\text{Na}$ reaction excitation function and its energy-dependent covariance matrix were re-evaluated in the energy range from threshold up to 60 MeV.

Excitation functions of the $^{27}\text{Al}(n,2n)^{26m}\text{Al}$ and $^{27}\text{Al}(n,2n)^{26g}\text{Al}$ reactions were evaluated for dosimetry applications for the first time.

Comments: Attendees of RCM-3 recommended the inclusion of the $^{23}\text{Na}(n,\gamma)^{24}\text{Na}$, $^{23}\text{Na}(n,2n)^{22}\text{Na}$, $^{27}\text{Al}(n,2n)^{26m}\text{Al}$ and $^{27}\text{Al}(n,2n)^{26g}\text{Al}$ reactions in the next version of the IRDFF library. The evaluation procedures are documented in IAEA report INDC(NDS)-0705 by K. Zolotarev (<https://www-nds.iaea.org/publications/>)

As a result of a joint discussion, the participants of RCM-3 recommended that new measurements be taken of the $^{23}\text{Na}(n,2n)^{22}\text{Na}$ cross sections at energies above 20 MeV, where existing data are still scarce and controversial.

3.2. Analysis and updating of the nuclear decay data evaluations to improve the IRDFF Decay sub-library, V. Chechev

Khlopin Radium Institute, Saint Petersburg, Russian Federation

The progress and status of the IRDFF decay data library were presented.

The decay data for 52 radionuclides, which are the dosimetry neutron reaction residuals, were considered between the 2nd and 3rd RCM of the CRP. The evaluated decay data contained in the IRDFF file before the start of the CRP in Oct 2012 were tested for validity and a list of radionuclides was defined for those that have newly published experimental data and/or important compilations available.

Using the Decay Data Evaluation Project (DDEP) methodology, the analysis of decay schemes and the full re-evaluation or update of decay data were performed for the radionuclides from the above list. Small update amendments were introduced, where needed, to the existing sets of ENSDF/DDEP evaluated data which mainly retain their validity.

All evaluated decay data were presented in the ENSDF format which was transferred into the ENDF format. As a result, there are currently modern evaluated decay data available for 72 radionuclides, which are the residuals of the IRDFF neutron dosimetry neutron reactions.

After this work, the IRDFF decay sub-library consists of 102 radioactive isotopes, 72 of which were updated during the CRP period. Among the remaining 30, 28 were taken from the latest ENSDF evaluations released during the last eight years.

Participants of RCM-3 recommend the creation of a compact table (as an extract from the IRDFF decay library) which lists the decay parameters (Q value, decay mode, half-lives, energies and intensities) for the prominent radiations which are typically used in the activation measurements.

Further essential improvements are still needed for the isotopes ^{94m}Nb and ^{194}Au , which are produced in the $^{93}\text{Nb}(n,\gamma)$ and $^{197}\text{Au}(n,4n)$ reactions, correspondingly.

The atomic masses should be taken from the latest mass evaluation AME, which are available at <https://www-nds.iaea.org/amdc/>.

Comments: The reliability of the absolute gamma-emission probabilities in the decay of ^{187}W was questioned. The recommendation in ENSDF differs from the old one by 20%. The analysis at IRMM of the TOF measurements could not be reconciled with the thermal capture cross section derived from activation measurements using the recommended gamma-emission probabilities. New measurements of the thermal neutron radiative capture cross section for the $^{186}\text{W}(n,\gamma)^{187}\text{W}$ reaction by the activation method with the use of current recommended gamma-ray emission probabilities resolve this discrepancy.

4. Nuclear Data Verification and Validation

4.1. Advanced UQ approaches to the validation of dosimetry cross sections in reactor benchmark fields: Input to 3rd RCM, P. Griffin

Sandia National Laboratories, Albuquerque, NM, USA

Summary of the progress made by Sandia National Laboratories in its support of the International Atomic Energy Agency (IAEA) Nuclear Data Section (NDS) Coordinated Research Project (CRP) on the testing and improving of the International Reactor Dosimetry and Fusion File (IRDF) was reported. A set of applicable uncertainty quantification (UQ) approaches for the analysis of the consistency of integral cross section measurements in neutron benchmark fields have been surveyed. It was concluded that for reactor fields, the best approach was a least-squares methodology that addressed the combined uncertainty from the neutron spectrum characterizing the benchmark field, the measured activity for the dosimetry reaction and the dosimetry cross section for which validation evidence was being sought. This least squares approach was then applied to the ^{252}Cf spontaneous fission standard benchmark field, the ^{235}U thermal fission reference benchmark field and to seven different reactor-based reference benchmark neutron fields, ranging from a highly enriched ^{235}U fast burst metal assembly to a moderated pool-type reactor field. This validation effort provided good validation evidence for 64 of the IRDF reactions. The $^{252}\text{Cf}(s.f.)$ field provided validation evidence for 46 reactions. The $^{235}\text{U}(th)$ field provided validation evidence for 50 reactions, 8 of which had not been validated in the $^{252}\text{Cf}(s.f.)$ standard benchmark field. The analysis of the reactor field included sensors with covers that shifted the energy range for the response of the dosimeters. When the best validation data gathered from these seven reactor fields were considered, reactor-based validation evidence existed for 40 reactions, from which 11 had not been validated in either the $^{252}\text{Cf}(s.f.)$ or $^{235}\text{U}(th)$ neutron fields. The investigation was concluded by identifying efforts to be pursued in reactors that could further enhance the validation of the IRDF dosimetry library and by identifying reactions where the community needs to look to accelerator-produced neutron fields for validation evidence.

Comments: The metrics surveyed for validation include:

- Spectrum-averaged cross sections (which can be sensitive to how well the spectra are known)
- Spectral indices, for which there exists a limited set of data

Least squares combined analysis (best approach for reactor fields)

In the $^{252}\text{Cf}(s.f.)$ field, measurement data was examined for 49 reactions. Problems were seen with the $^{59}\text{Co}(n,\gamma)$ and $^{92}\text{Mo}(n,p)$ reactions. The initial least-square-based spectrum adjustment used 47 different reactions and provided a good chi²-per-degree-of-freedom of 1.43. The analysis of the data in this neutron field provided validation evidence for 46 of the IRDF reactions. In addition to the $^{59}\text{Co}(n,\gamma)$ and $^{92}\text{Mo}(n,p)$ reactions, poor validation evidence was also seen for the $^{232}\text{Th}(n,f)$ reaction. Validation evidence for the $^{27}\text{Al}(n,p)$ and $^{60}\text{Ni}(n,p)$ reactions was acceptable, but these reactions provided the largest contributions to the chi-square in this neutron field. The measured spectrum averaged cross section for the $^{46}\text{Ti}(n,2n)$ reaction had very large uncertainties, which led to designating the validation evidence for this reaction as marginal.

The measurements for the $^{10}\text{B}(n,\alpha)$ and $^6\text{Li}(n,t)$ reactions are typically based on the use of helium accumulation fluence monitors (HAFMs). The irradiation of boron and lithium have helium contributions that can arise from other alpha production channels, which also need to be included in future versions of the IRDFF library. In addition, future IRDFF libraries should include a cross section for the total helium and for the total tritium production in the naturally occurring boron and lithium isotopes.

In the $^{235}\text{U}(\text{th})$ neutron field, the HAFM measurements for the $^{10}\text{B}(n,\alpha)$ and $^6\text{Li}(n,t)$ reactions required large corrections, i.e., 0.81 for B and 0.71 for Li, to account for the helium contributions from these other channels. This large correction called the validation evidence for these reactions in the $^{235}\text{U}(\text{th})$ field into question.

Recent corrections to the measured $^{64}\text{Zn}(n,p)$ activity, which reflect the updated gamma emission probabilities, reported in the measurement for the $^{235}\text{U}(\text{th})$ field should be reflected in an update of this work for the $^{235}\text{U}(\text{th})$ field.

The SPR-III fast burst ^{235}U reactor provided validation evidence for many reactions in the fast energy range that had not been validated in the $^{252}\text{Cf}(\text{s.f.})$ or $^{235}\text{U}(\text{th})$ fields.

The proposed new draft of ASTM E1018-17 standard for the selection of dosimetry cross sections for use in support of surveillance dosimetry in light water reactors endorses the IRDFF library for all of the relevant dosimetry reactions.

4.2. Benchmarking of IRDFF against 14 MeV neutronics experiments at ENEA Frascati, M. Angelone

Division of Fusion Centro Ricerche Energia, Frascati, Italy

ENEA activities on IRDFF testing and validation are mainly focussed on validating the IRDFF file at neutron fusion relevant energy (14 MeV). ENEA mainly uses the IRDFF file in substitution of the old IRDF-2002 file for dosimetry calculation (reaction rates) in nuclear analysis of tokamak and in fusion neutronics benchmark and mock-up experiments.

The new activities of ENEA were mainly focused on the analysis of a copper benchmark experiment performed at FNG in 2015. The benchmark consisted of irradiation with 14 MeV neutrons of a $60\times 60\times 70\text{ cm}^3$ block of pure OFC copper (oxygen free). Several different measurements were carried out, such as: a) reaction rate measurements in seven different penetration depths along the mid-plane of the block, b) neutron and gamma flux spectra measurements in two positions inside the Cu block, and c) dose measurements in different positions inside the block by thermoluminescent dosimeters (TLD).

For the purposes of the present meeting, ENEA compared the reaction rates (RR) calculated inside the Cu block using IRDF-2002 and IRDFF_v1.05 dosimetry files. The nuclear responses were calculated with the MCNP5 code using JEFF-3.1.1/JEFF 3.2 and FENDL3 nuclear data library for transport. The activation reactions used were: $^{93}\text{Nb}(n,2n)^{92\text{m}}\text{Nb}$, $^{197}\text{Au}(n,2n)^{196}\text{Au}$, $^{27}\text{Al}(n,\alpha)^{24}\text{Na}$, $^{58}\text{Ni}(n,p)^{58}\text{Co}$, $^{115}\text{In}(n,n')^{115\text{m}}\text{In}$, $^{186}\text{W}(n,\gamma)^{187}\text{W}$, $^{197}\text{Au}(n,\gamma)^{198}\text{Au}$ and $^{55}\text{Mn}(n,\gamma)^{56}\text{Mn}$ which cover the whole neutron energy range for fusion neutronics.

The comparison between the RR calculated with IRDF-2002 and IRDFF_v1.05 addressed the following points:

- For all the threshold reactions, the results calculated using IRDF-2002 and IRDFF_v1.05 are almost the same within $\pm 1\text{-}2\%$ (Max). Larger discrepancies are observed for thermal sensors.
- The IRDFF_v1.05 results *are lower compared to* the IRDF-2002 (v-2005) results for $^{186}\text{W}(n,\gamma)$ by about 20% (constant difference with penetration depth)
- The IRDFF_v1.05 results *are higher compared to* the IRDF-2002 results for $^{55}\text{Mn}(n,\gamma)$ by about 10% (constant trend with penetration depth). The trend is consistent with the increase of the capture cross section in the resonance region of IRDFF V1.05.

The causes of the observed discrepancies are under investigation. However, it could be attributed to the observed differences in the thermal reaction cross section between the old IRDF-2002 and the new

IRDFFF_v1.05 files. Differences in the centroid, width and height of the resonances have been observed for the used thermal sensors. A deeper analysis of the calculated RR has been performed by taking the ratio of the bin-to-bin calculated thermal RR (MCNP calculations were performed using the VITAMIN-J structure).

4.3. Final results of IRDFFF benchmark experiments at JAEA/FNS, C. Konno

Japan Atomic Energy Agency, Ibaraki-ken, Japan

The Fusion Neutronics Source (FNS) facility of JAEA reported the final results for the following parameters: (i) the comparison between IRDFFF v1.05 and previously measured cross sections for 38 reactions around 14 MeV (ii) the reaction rate measurement for 41 reactions inside the graphite assembly, where there are a lot of low energy neutrons, (iii) the reaction rate measurement inside the Li₂O assembly, where there are few low energy neutrons. An additional reaction rate measurement inside the graphite assembly was also carried out for 5 reactions, where half-lives of produced radioisotopes are shorter than ~ 40 min. The IRDFFF excitation functions in most cases agree well with the activation cross-sections measured at FNS in the energy interval 13.3 to 15 MeV, though some disagreement is observed for ²⁹Si(n,x)²⁸Al, ⁴⁸Ti(n,x)⁴⁷Sc, ⁶⁴Zn(n,p)⁶⁴Cu and ¹¹³In(n,n')^{113m}In. The graphite and Li₂O experiments indicate agreement between the measured reaction rates and calculated ones with IRDFFF v1.05 within 10% for most reactions. It is concluded that IRDFFF v1.05 is generally good. It is requested that the elastic cross section data be added to the ⁵⁵Mn, ⁵⁸Fe, ²³⁵U and ²³⁸U files in IRDFFF.

Comments: K. Zolotarev noted that the observed disagreements for the ⁶⁴Zn(n,p) reaction are mainly caused by not using the recommended gamma emission probabilities for ⁶⁴Cu in IRDFFF.

4.4. Improvements to STAYSL PNNL spectral adjustment with IRDFFF, L.R. Greenwood

Pacific Northwest National Laboratory (PNNL), Richland, WA, USA

The STAYSL PNNL program performs a least-squares adjustment of the neutron spectrum based on the IRDFFF cross section library and user-defined activation data and a starting neutron spectrum. All known covariances are included. Required corrections are included for the irradiation history, gamma absorption, neutron burn-up, and neutron self-shielding using separate utility programs prior to the execution of STAYSL PNNL. Neutron cross section libraries based on IRDFFF V1.05 to 60 MeV are provided including 69 (WIMS), 129 (14 MeV), 140 (prior 100 groups extended to 60 MeV), 175 (Vitamin J), 640 (old SANDII to 20 MeV), and 725 (old SAND II extended to 60 MeV) energy groups. Five new reactions were included in IRDFFF V1.05, namely SI28P, MN552, CO593, CO59P, ZN67P, MO92P, IN113N, IN113G, TM1693, BI2093, U235G, and U2382 (in STAYSL nomenclature for the reactions). Calculations are included to demonstrate the need for activation cross sections from natural targets such as ^{nat}Ti(n,x)⁴⁶Sc rather than only from isotopic targets such as ⁴⁶Ti(n,p)⁴⁶Sc and ⁴⁷Ti(n,x)⁴⁶Sc. The effects of such reactions increase dramatically with increasing neutron energies and cannot be neglected. Some important reactions such as ⁵⁶Fe(n,x)⁵⁴Mn are not currently included in IRDFFF and prevent the use of the ⁵⁴Fe(n,p)⁵⁴Mn reaction as a monitor at higher neutron energies. It is recommended that natural element cross sections be included in future releases of IRDFFF for a list of reactions that suffer from reactions on multiple isotopes that lead to the same activation product. Spectral adjustments are illustrated on Be(d,n) thick target neutron fields at deuteron energies of 30 and 40 MeV.

Comments: Integral testing of IRDFFF cross sections has been performed in a variety of high energy neutron fields such as Be(d,n) thick targets irradiated with deuterons at 30 and 40 MeV. The neutron spectra were characterized by neutron time-of-flight measurements. The data will be added to EXFOR if not already included. These data can be used to validate IRDFFF cross sections at higher neutron energies. At higher neutron energies, elements with multiple isotopes have competing reactions for the production of specific activation products. Elemental activation cross sections are thus needed in order to use these reactions for neutron spectral adjustment. Six reactions have the required files in IRDFFF, but there are many cases where new evaluations may be needed to provide the missing data.

4.5. Analysis of ASPIS-IRON88 benchmark and TRIGA measurements for IRDF validation and proposals for the REAL-201X adjustment exercise, I. Kodeli

Jožef Stefan Institute, Ljubljana, Slovenia

Within the scope of the IRDF validation program of the IAEA, a detailed analysis of the mild steel shielding benchmark ASPIS-Iron88 was performed at the JSI to compare the performance of the new IRDF library against the previous IRDF-2002 data and to verify the progress made. ASPIS-Iron88 benchmark (described in the SINBAD package NEA-1517/75) consisted of a 67 cm thick iron block placed behind a graphite column and a fission plate, irradiated in a ^{235}U fission spectrum. Several reaction rates were measured and calculated using the MCNP and DORT codes: $^{27}\text{Al}(n,\alpha)$, $^{103}\text{Rh}(n,n')$, $^{115}\text{In}(n,n')$, $^{32}\text{S}(n,p)$ and $^{197}\text{Au}(n,\gamma)$. The analysis included the cross-section sensitivity and uncertainty analysis, using the SUS3D code, and the adjustment exercise, using the newly developed code by Lucijan Plevnik at JSI. Adjustments to IRDF response functions were also calculated, as well as the transport cross-sections and fission spectra.

A similar analysis is under way for the recent FNG-Copper benchmark, but the quality of the recent copper transport data does not yet allow conclusions to be made on the quality of the IRDF data.

TRIGA Reactor experimental data sets were considered and proposed by JSI for the REAL-201X Neutron Spectral Adjustment Exercise, including six (bare and covered) reaction rates: $^{27}\text{Al}(n,p)$, $^{197}\text{Au}(n,\gamma)$, $^{45}\text{Sc}(n,\gamma)$, $^{55}\text{Mn}(n,\gamma)$, $^{58}\text{Fe}(n,\gamma)$, $^{59}\text{Co}(n,\gamma)$ and $^{232}\text{Th}(n,\gamma)$, which were measured in the irradiation channel F24 located at the periphery of the reactor core. The initial spectrum in the channel F24 was calculated using a detailed (verified and validated) computational model of the JSI TRIGA reactor developed using the Monte Carlo code MCNP5. Spectra calculated using MCNP are provided for use as a prior.

New measurements of the $^{55}\text{Mn}(n,\gamma)$ reaction at several locations in the TRIGA reactor are under preparation for this spring.

Proposed REAL Exercise

The proposal for a new REAL neutron spectrum-unfolding exercise was discussed. The outlines of the project were defined but the exercise cannot be carried out within the scope of the current CRP. Thirteen cases were selected for the exercise covering fission reactors, critical benchmarks, fusion benchmarks, and neutron time-of-flight spectra. For most of the cases, the necessary input data are collected although more work is needed on covariances for the input neutron spectra. Further details are on the dedicated web page <https://www-nds.iaea.org/REAL/>.

The RCM-3 participants recommend that the REAL exercise should be considered by the IAEA in the future.

5. Actions

5.1. Status of Actions from the 2nd RCM for the Improvement of IRDF

The $^{117}\text{Sn}(n,n')^{117\text{m}}\text{Sn}$ (14 day half-life) reaction would be useful to include in HPRL since it is a unique way to measure neutrons in the 300 keV energy range.

Action: NDS (S. Simakov), All

DONE. A proposal for an entry into the HPRL was submitted to the NEA Data Bank.

Participants agree that the set of reactions that need to be updated or require new evaluations that are included in the IRDF database are $^{23}\text{Na}(n,\gamma)$, $^{23}\text{Na}(n,2n)$, and $^{27}\text{Al}(n,2n)$.

Action – K. Zolotarev

DONE. Draft report is available, revision of the $^{23}\text{Na}(n,2n)$ reaction cross sections is expected by the end of April 2018 to reflect comments expressed at the Meeting.

There are several cases where isotopic or natural element (n,x) reaction data would be highly useful. Examples include $^6\text{Li}(n,x)^4\text{He}$, $^7\text{Li}(n,x)^3\text{H}$, $^7\text{Li}(n,x)^4\text{He}$, $^{10}\text{B}(n,x)^4\text{He}$, $^{11}\text{B}(n,x)^4\text{He}$, $^{\text{nat}}\text{Ti}(n,x)^{46}\text{Sc}$, $^{\text{nat}}\text{Ti}(n,x)^{47}\text{Sc}$, $^{\text{nat}}\text{Ti}(n,x)^{48}\text{Sc}$, $^{\text{nat}}\text{Zn}(n,x)^{67}\text{Cu}$, $^{\text{nat}}\text{Fe}(n,x)^{54}\text{Mn}$ and all cases where there are significant differences between the activation of elemental and isotopically-enriched targets or where there are additional reaction channels at higher neutron energies leading to the same residual isotope.

Partial cross sections for different isotopes need to be summed to create the elemental files.

Action: NDS, L. Greenwood

Reactions were identified in the presentation: 6 are already available in IRDFF; 10 are to be evaluated and added if possible.

There is a significant discrepancy on the $^{55}\text{Mn}(n,\gamma)$ cross section from 10 keV to 1 MeV that needs to be addressed. Experiments at FNG will be useful in this regard. FNS will perform measurements to validate this reaction in the W bulk experiment.

Action: M. Angelone, C. Konno, I. Kodeli

Results from JAEA were provided for the Li_2O experiment, but not for a tungsten experiment because the facility was shut down.

The $^{58}\text{Fe}(n,\gamma)$ reaction, as well as many other capture reactions, tend to be discrepant in the 10 keV to 1 MeV energy region for fast reactor, shielding, and fusion applications. The FNS experiments will provide data on some of the reactions that were measured.

Action: C. Konno

The experiment could not be performed because the facility was shut down. The action has been dropped.

More measurements and validation are needed in the higher neutron energy range above 20 MeV. Experiments are in progress for Bi and Co. A comparison exercise is planned on more experiments at common neutron energies around 40 MeV for data evaluations.

Action: M. Majerle, H. Yashima, R. Nchodu

Majerle, NPI Rez: Experiments were performed but more work is needed to determine the low-energy tail corrections;

Yashima, Kyoto University: beam time was not available for the additional experiments at lower energies;

Ndlovu, iThemba LABS: experiments are planned for May 2017.

We encourage more measurements of some IRDFF reactions in well-characterized ^{252}Cf neutron fields. Such sources exist or are planned in EPFL, CV (Research Center) Rez, NPL (UK), and Institute of National Standards. In particular, measurements are needed on high threshold reactions such as (n,2n) or (n,3n) to reduce uncertainties on the higher energy part of the ^{252}Cf neutron spectrum.

Action: NDS, C. Destouches, A. Plompen

Some results were already published, new measurements are in progress at Rez, A measurement on ^{89}Y will be completed by September 2017.

A. Plompen's request for funding in 2016 for an experiment at NPL was not awarded; it is therefore unlikely that any further activity will be undertaken by JRC-Geel for this neutron field.

Re-evaluations of previous experiments are needed to resolve some discrepancies for the ^{235}U PFNS field at neutron energies above 10 MeV. New measurements are encouraged to assist in improving the database. Potential facilities are BR1 (Mol), FRM2 (Munich), Budapest Research Reactor, NIST, Kyoto, and ILL. 15

Action: A. Plompen

New measurements at Rez in LR-0 reactor field on ^{90}Zr (n,2n), ^{75}As (n,2n), ^{23}Na (n,2n) and ^{89}Y (n,2n) are finalized and may serve for the purpose of data validation in combination with measurements in the ^{252}Cf spontaneous fission neutron field. A paper on ^{90}Zr (n,2n) and ^{89}Y (n,2n) SPA cross sections was sent for publication and is under the review process. A. Plompen, A. Wallner, R. Capote are scheduling an experiment at ILL for the fall of 2017.

Los Alamos is encouraged to continue to investigate and report the data and methods, particularly the expected uncertainties, associated with the historic critical assembly activation measurements. Planned new measurements in bare and natural uranium reflected highly-enriched uranium critical assemblies, particularly to obtain IRDFF activations that are not measured, would be very valuable.

Action: M. White

M. White could not attend the Meeting, but a consultancy visit at the IAEA is planned where the issues of reaction rate ratio measurements will also be discussed.

IRDFE should include some warnings on known problems such as the branching ratio to ^{58g}Co vs. ^{58m}Co from the $^{58}\text{Ni}(n,p)$ reaction and for ^{196g}Au vs. ^{196m}Au from the $^{197}\text{Au}(n,2n)$ reaction. Energy-dependent branching ratios for ^{58}Co should be added to IRDFE in order to support calculations of burnup during reactor irradiation.

Action: NDS

The action is still pending; NDS will investigate the possibility to evaluate the excitation functions for the production of the isomers.

There are disagreements between JEFF and IRDFE evaluations for $^{237}\text{Np}(n,f)$ and $^{241}\text{Am}(n,f)$ measurements between LANL and n-TOF in the plateau region from 2.5 keV to 100 keV energy range, and for $^{237}\text{Np}(n,\gamma)$ measurements in the 100 keV to 2 MeV energy range that need to be resolved.

Action: V. Pronayev, K. Zolotarev, G. Noguere

The paper published by M. Diakaki in 2016 on a new evaluation of the $^{237}\text{Np}(nf)$ cross section evaluation made at n-TOF might give valuable information for ^{237}Np fission cross section and should be checked. The rest of the action is still pending.

There is a 15% discrepancy between the IRDFE and measured spectrum averaged cross section for $^{238}\text{U}(n,2n)$ in the ^{235}U thermal neutron-induced PFNS field. The reason could be due to the contribution from the competing reaction (γ,n) which also leads to ^{237}U . A similar problem may exist with (n,f) and photo-fission reactions for ^{238}U . Additional effort is needed to simulate such experiments and to determine how to properly use current nuclear data. Validation of photonuclear data on SINBAD benchmarks with MCNP will be done.

Action: NDS, I. Kodeli

S. Simakov reported on the (γ,f) contribution, which amounts to 1% for an ideal case of fission in a thin ^{235}U foil. The action on I. Kodeli has been dropped because the available SINBAD benchmarks were found to be unsuitable to resolve the above-mentioned discrepancies; new measurements of the $^{238}\text{U}(n,2n)$ cross sections were performed at TUNL university, USA, and are included in the new ^{238}U IAEA-CIELO evaluation. The integral measurement seems to be in error.

A verification of the MACS results for $^{238}\text{U}(n,\gamma)$ and $^{197}\text{Au}(n,\gamma)$ is recommended. There are new measurements by AMS (Wallner) that have to be considered.

A re-measurement of the $^{55}\text{Mn}(n,\gamma)$ reaction and comparison with neutron TOF data is needed. The $^{55}\text{Mn}(n,\gamma)$ measurements should be considered as a test case for this mass range.

Action: P. Mastinu, A. Plompen

It was noted that the official Kadonis data base for MACS at 30 keV still recommends values, many of which were normalised to their internal gold standard of 582 mb, which is known to be too low. The Wallner measurements for ^{197}Au and ^{238}U are included in the new Standards to be released in 2017 and they predict a higher value of 618 mb for the MACS of ^{197}Au . There is a new "test" version of the Kadonis data base <http://exp-astro.physik.uni-frankfurt.de/kadonis1.0> which gives the value 612.8(7.0) mb for ^{197}Au that exactly matches the ENDF/B-VII.1 value. This is lower than the value from the new Standards, but within the uncertainty band. Note that in Astrophysics the spectrum is defined in the centre-of-mass coordinate system; the 30 keV spectrum corresponds to the spectrum in the Lab system shifted by a factor $(A+1)/A$, which for gold corresponds to 30.15 keV. For the light elements the difference is much more significant.

A measurement under B_4C cover in SPR-III facility, reported by P. Griffin, did not reveal any significant discrepancy that would affect MACS of the $^{55}\text{Mn}(n,\gamma)$ reaction.

A. Plompen reported that a measurement for $^{209}\text{Bi}(n,\gamma)^{209g}\text{Bi}$ was performed at the SARAF facility of SOREQ, Israel (A. Shor et al., ND2016). A preliminary result shows a lower cross section than that of Kadonis for the 30 keV MACS. The result will be published in 2017.

In the frame of the CRP, the decay data library is being updated and all participants are strongly encouraged to use this library for consistency and document any differences with prior experiments.

New experimental activation data should include full documentation of the experiment (half-life, gamma intensities, counting times, irradiation time, cooling times, reference reactions) and other data that are required for the later re-evaluation of the measurements.

Nuclear decay data problems were identified for the following nuclides:

- ^{103m}Rh - x-ray emission probability around 20 keV
- ^{140}La - gamma intensities for lines below 1596 keV
- ^{187}W - gamma intensities of 2 lines (473.53 keV and 685.81 keV)
- ^{64}Cu - 511 keV annihilation gamma line intensity tends to be increased essentially

Action: V. Chechev, All

V. Chechev presented an updated decay data library, which is available in ENDF-6 format for IRDFF; new measurements of X-ray emission probability for ^{103}Rh had been performed by CEA/LNHB, France, and are expected to be published before the end of 2017. The current entries in the library will be checked against the new measurements.

5.2. New Actions Emerging from the Discussions during the 3rd RCM

1. Merge particle-production cross sections and covariances into elemental data for reactions that are already available in IRDFF.
Action: NDS will do the merging into elemental data for reactions that are already present in IRDFF, namely $\text{Si}(n,x)^{28}\text{Al}$, $\text{Ti}(n,x)^{46}\text{Sc}$, ^{47}Sc , ^{48}Sc , $\text{Cu}(n,x)^{64}\text{Cu}$ and $\text{In}(n,x)^{114m}\text{In}$.
Action: NDS will check the status of other channels contributing to alpha-production and tritium-production on ^{10}B and Li (end of 2017).
2. Evaluate secondary reactions that are needed to reconstruct the particle-production cross sections and covariances at higher energies, identified by L. Greenwood.
Action: K. Zolotarev – provide a list of reactions that can possibly be evaluated and the time frame for completion of the work (April 2017).
3. Check the IRDFF MACS cross sections against the updated Kadonis data base.
Action: S. Simakov – check MACS against the updated Kadonis data base (April 2017 IRDFF_v1.05, November 2017 for IRDFF-2.0).
4. An update to the IRDFF-1.05 library should be released, named IRDFF-2.0
Action: NDS – assemble and release the new library (end of 2017).
5. The new Standards evaluations have been completed and will be released before the end of 2017. They are included in the IAEA-CIELO evaluations and in the candidate evaluations for the ENDF/B-VIII library, which will be released before the end of 2017.
Action: NDS – include IAEA-CIELO or ENDF/B-VIII evaluations (which are consistent with the Standards) for reactions relevant to IRDFF (to be included in IRDFF-2.0).
6. Experimental SACS were measured in the LR-0 reactor for the $^{75}\text{As}(n,2n)$; $^{90}\text{Zr}(n,2n)$; $^{89}\text{Y}(n,2n)$ and $^{23}\text{Na}(n,2n)$ reactions, together with the neutron spectrum of the irradiation facility.
Action: M. Kostal – provide a report containing a brief description of the experiment and the numerical data for the measured values and the spectrum (July 2017).
7. Experimental SACS were measured in the Cf(s.f) field in Research Center Rez for the $\text{Fe-54}(n,p)$; $\text{Fe-54}(n,\text{alfa})$; $\text{Na-23}(n,2n)$; $\text{Al-27}(n,p)$; $\text{Al-27}(n,\text{alfa})$; $\text{F-19}(n,2n)$; $\text{Zr-90}(n,2n)$ and $\text{Y-89}(n,2n)$ reactions.
Action: M. Schulc – provide a report containing a brief description of the experiment and the numerical data for the measured values (July 2017).
8. Several reference neutron fields were identified. They must be assigned unique 4-digit identification numbers and entered into the IRDFF spectra file.
Action: P. Griffin – provide spectra for 7 neutron fields defined at SNL (May 2017).
Action: M. Kostal – provide spectrum in “Special cores (void and graphite case)”, which is proposed as an IRPhEP benchmark (June 2017).

- Action: S. Simakov – provide recalculated spectra in 640 groups for the ISNF neutron field and the spectra from the old IRDF2002 library (June 2017).
- Action: NDS – obtain the spectrum from the NIST RT-2 facility (April 2017).
- Action: I. Kodeli – provide spectrum from the TRIGA reactor at JSI (April 2017).
9. Elastic cross sections are needed with resonant cross section for the purpose of calculating self-shielding with codes like NJOY.
Action: NDS will add elastic cross sections to complement capture cross sections with resonance structure (end of 2017).
 10. There exist measurements in spectra with average energies above the conventional fission spectra, which could be used for the validation of the dosimetry reactions at higher energies.
Action: L. Greenwood will provide measured activation rates and detailed spectra for inclusion in EXFOR that are not included yet (July 2017).
 11. The Kayzero database can serve as an important independent source of data for the validation of the thermal capture cross sections and resonance integrals.
Action: NDS will perform the comparison of thermal cross sections and resonance integrals with the data derived from the Kayzero library for the IRDF-2.0 library (November 2017).
 12. Fission product yields are needed in some applications related to neutron dosimetry. A recommendation on the choice of evaluations is needed.
Action: P. Griffin and L. Greenwood will check the document INDC(NDS)-0713 and convey a recommendation on the choice of fission product yield data (May 2017).
 13. DPA data were traditionally included in the dosimetry library. By default, the original data are to be adopted for IRDF-2.0.
Action: S. Simakov will provide the results of their most recent calculations of iron DPA for possible addition to the IRDF-2.0 library (November 2017)
Action: P. Griffin will provide displacement kerma for Si that are consistent with the new ASTM standard.
 14. New measurements were done at iThemba LABS on Bi at 90 MeV and 140 MeV.
Action: N. Ndlovu – Submit the final results for Bi to the IAEA by June 2017.
 15. Evaluation of Bi up to 100 MeV was performed by V. Pronyaev. Considering that new measurements are available up to 140 MeV, the evaluation could be extended to a higher energy.
Action: V. Pronyaev – consider extending the evaluation of Bi up to 140 MeV.

6. Outline of the Final CRP Report

Objectives

New IRDFF-2.0 library

- List of contents
 - Reaction cross section data (S. Simakov: help with the assembly of the list with links to the original documents).
 - Reference neutron fields (P. Griffin: assemble the list of reference neutron fields)
 - Decay data (V. Chechev)
 - FPY (P. Griffin)
 - DPA (S. Simakov)

What is new since IRDFF-1.00

- Extension to 60 MeV (NDS)
- New materials/reactions (NDS: check the list of documents by K. Zolotarev, new evaluations for Standards and CIELO)
- Re-evaluated reactions (NDS)
- Updated/Extended library of reference neutron fields (P. Griffin)
- Updated decay data library (V. Chechev)
- New differential measurements specifically above 20 MeV (Yashima, Ndlovu, Majerle)
- New integral measurements for data validation (Cf252sf, U235tf, Reactor spectra, FNS, Kostal, Destouches, Konno)
- Compilation of older measurements for EXFOR and the library of reference neutron fields at high energies (Greenwood)

Summary of the validation results

- Thermal cross sections and RI (NDS)
- Cf252sf, U235tf (Simakov, Griffin, Kostal)
- MACS (Simakov)
- Reactor-related neutron fields (Kostal, Destouches, Griffin, LANL)
- Fusion-related spectra (Konno)
- High-energy neutron fields (Greenwood)

Utilities

- SDF2NDF (Verpelli)
- STAYSL PNNL (Greenwood)
- RR_UNC (NDS)
- COVEIG (NDS)
- CALMAR (G. Gregoire, EPJ Web of Conferences 106, 07006 (2016), Available from the NEA Data Bank)
- Recommended template for storing/reporting activation measurements (NDS).

7. Participants' Summaries

7.1. Manage and technical contribution of NDS to CRP on the IRDFF testing, improving and validation, S. Simakov

Institute for Neutron Physics and Reactor Technology, Karlsruhe Institute for Technology, Germany

The Nuclear Data Section of the IAEA coordinated the joint technical work of CRP by identification and formulation of the differential and integral cross sections and their uncertainties for dosimetry reactions. For this the lists of *Reactions to Measure* (this list was also submitted to the High Priority Request List of the NEA Data bank) and *Reactions to Update/Evaluate* were created and regularly updated to follow the current requests from the fission, fusion and spallation applications.

The staff of NDS also made technical contributions to this CRP. This summary describes several such studies, more information is available on the *CRP web-page*.

Collecting the old and new measured data relevant to this CRP in the EXFOR database.

The old measurement data relevant to the improving and validation of IRDFF were identified and assigned for compilation in EXFOR. Such data included around 15 sets of differential and integral *Cross Sections* (see also *NRDC Memo CP-D/836*) and more than 20 with Neutron *Sources Spectra*. The newly measured and published data are timely compiled in EXFOR in accordance with the NRDC rules and practice.

Assembling and releasing of the IRDFF cross sections sub-library. The releases of the IRDFF cross sections are reflected in the regularly updated *List of Reactions or Table 4* which protocols the progress since IRDFF-1.0 (see *INDC(NDS)-0616*, May 2012):

- IRDFF-1.03 (Mar 2014) included new reaction $^{238}\text{U}(n,2n)^{237}\text{U}$ and updates of $^{54}\text{Fe}(n,p)^{54}\text{Mn}$, $^{58}\text{Ni}(n,2n)^{57}\text{Ni}$, $^{93}\text{Nb}(n,\gamma)^{94}\text{Nb}$, $^{115}\text{In}(n,\gamma)^{116\text{m}}\text{In}$ (K. Zolotarev, *INDC(NDS)-0657*<https://www-nds.iaea.org/publications/indc/indc-nds-0657.pdf>, Dec 2013);
 - IRDFF-1.04 (Nov 2014) included minor format corrections compared to IRDFF-1.03;
 - IRDFF-1.05 (Oct 2014) included new reactions $^{28}\text{Si}(n,p)^{28}\text{Al}$, $^{29}\text{Si}(n,x)^{28}\text{Al}$, $^{113}\text{In}(n,\gamma)^{114\text{m}}\text{In}$ and updates of $^{31}\text{P}(n,p)^{31}\text{Si}$ (K. Zolotarev, *INDC(NDS)-0668*<https://www-nds.iaea.org/publications/indc/indc-nds-0668.pdf>, Oct 2014);
 - currently are also evaluated new reaction $^{27}\text{Al}(n,2n)^{26\text{g}}\text{Al}$, $^{27}\text{Al}(n,2n)^{26\text{m}}\text{Al}$ and updated $^{23}\text{Na}(n,\gamma)^{24}\text{Na}$, $^{23}\text{Na}(n,2n)^{22}\text{Na}$ (K. Zolotarev, *INDC(NDS)*<https://www-nds.iaea.org/publications/indc/indc-nds-0668.pdf>)-<https://www-nds.iaea.org/publications/indc/indc-nds-0705.pdf><https://www-nds.iaea.org/publications/indc/indc-nds-0668.pdf>, in preparation, and contribution to RCM-3);
- for the higher energy (< 100 MeV) neutron dosimetry the new reactions $^{209}\text{Bi}(n,xn)^{210-x}\text{Bi}$, $x = 4 - 10$, were evaluated by V. Pronayev (see his *presentation* at RCM-2 in March 2015 and ENDF-6 formatted *file*).

Extension up to 60 MeV (if needed) of the new and updated evaluated files and their processing with PREPRO, RR_UNC, NJOY-2012 and MCNP codes was done by A. Trkov and S. Simakov. Discovered discover bugs in files and codes were fixed by A. Trkov, A. Kahler and O. Cabellos.

The releases of the ENDF-6 formatted IRDFF were made available for external usage at *CRP web-page* and *IRDFF web-page*.

As an outcome of CRP we expect a release of IRDFF-2.0 with at least 81 reactions, i.e. 6 new and 11 updated reactions compared to IRDFF-1.0 released before this CRP.

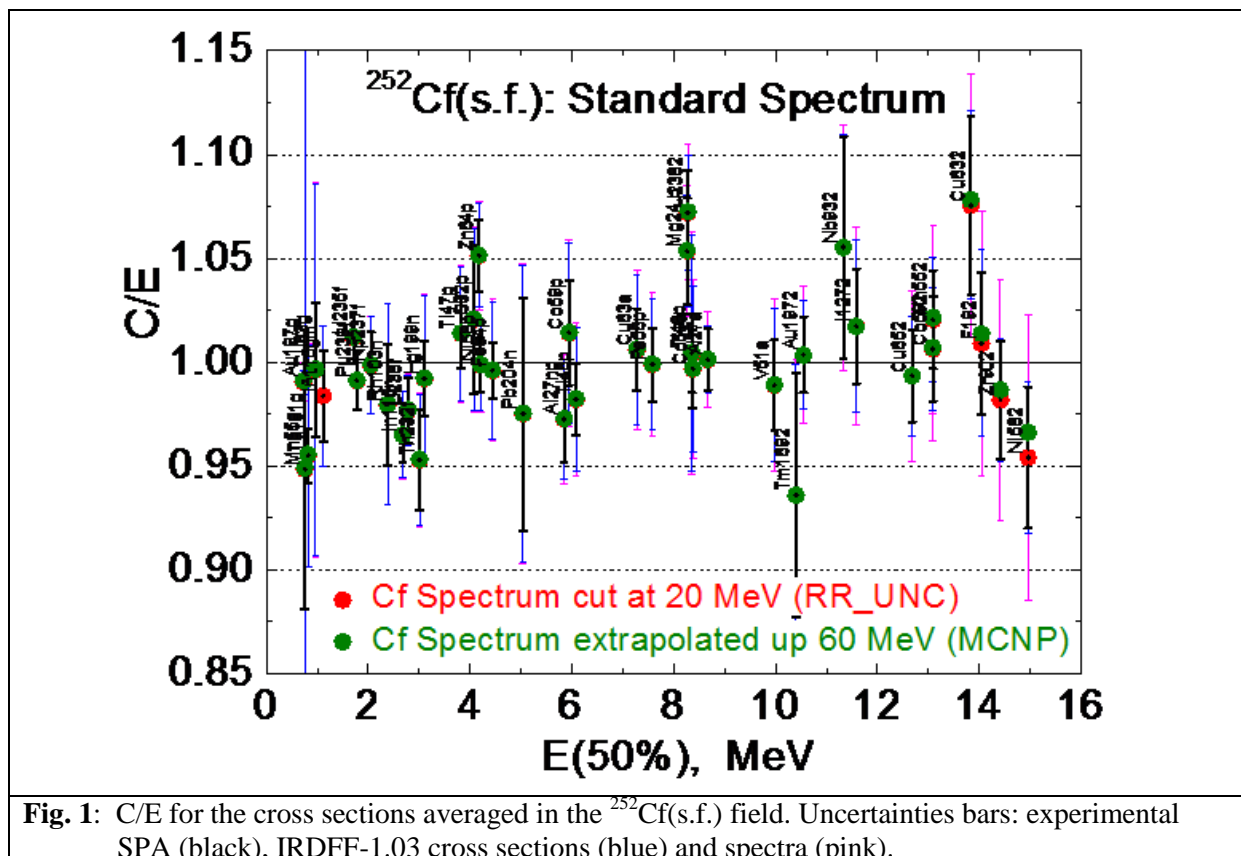
Assembling and releasing of the IRDFF decay data sub-library. Before start of CRP in 2012 the evaluated decay data for 82 isotopes were assembled from the ENSDF evaluations and made available in ENDF-6 formatted file *irdf2012.endf*. During CRP the analysis of decay schemes and the full re-evaluation or update of decay data were performed for many radionuclides by V. Chechev (see his contribution to RCM-3) using the Decay Data Evaluation Project (DDEP).

Consequently the list of radioactive isotopes was extended following the inclusion of new reactions in the IRDFF cross section sub-library. Eventually the IRDFF decay database will consist of 102 radioactive isotopes, 70 of which were updated during the CRP period.

The evolution and final stage of IRDFF decay sub-library is reflected on the dedicated CRP web-subpage [Actual Status and Needs for Decay Updating](#).

Collecting of known measured spectrum averaged cross sections (SPA) and using them for validation of the actual versions of IRDFF. This was done for (for more details see S. Simakov et al. [EPJ Web of Conferences 106\(2016\)04011](#)):

- $^{252}\text{Cf}(\text{s.f.})$ standard field: (*recommended*) *measured SPA*, IRDFF-1.03 *calculated SPA*, validation in terms of C/E ratios is shown in Fig. 1. Re-analysis employing the new measurements (see contribution of M. Kostal et al. to RCM-3) and IRDFF-1.05 will be done;
- $^{235}\text{U}(\text{n}_{\text{th}},\text{f})$ reference field: (*recommended*) *measured SPA*, IRDFF-1.03 *calculated SPA*, C/E ratios are displayed in Fig. 2. Re-analysis employing the new measurements (see contribution of M. Kostal et al. to RCM-3), $^{235}\text{U}(\text{n}_{\text{th}},\text{f})$ PFNS from ENDF/B-VIII and IRDFF-1.05 will be done;
- Reactor benchmark reference fields available in IRDF-2002 collection: the results of the C/E ratio analysis are shown in Fig. 3. Beforehand the *IRDF-2002 reference spectra* were checked, the ISNF facility was re-simulated to eliminate errors in spectrum, the correspondence between spectra and SPA presented in EXFOR was established. The ISNF spectrum will be however re-simulated to take into account the latest recommended $^{235}\text{U}(\text{n}_{\text{th}},\text{f})$ spectrum and neutron transport data from ENDF/B-VIII;
- Maxwellian ($kT = 30$ keV) reference field: the recommended measured SPA were taken from the latest version of *Kadonis-1.0* (used gold standard $^{197}\text{Au}(\text{n},\gamma) = 612.8 \pm 7.0$ mb) and for comparison from the previous version *Kadonis-0.3* (used gold standard $^{197}\text{Au}(\text{n},\gamma) = 582 \pm 9$ mb), the *calculated SPA from IRDFF-1.05* https://www-nds.iaea.org/IRDFF/listings/rr_unc_9228.pdf. Obtained C/E ratios for 15 IRDFF reactions are displayed in Fig. 4, only reaction $^{232}\text{Th}(\text{n},\gamma)$ is not validated in the Maxwellian-30keV benchmark yet.



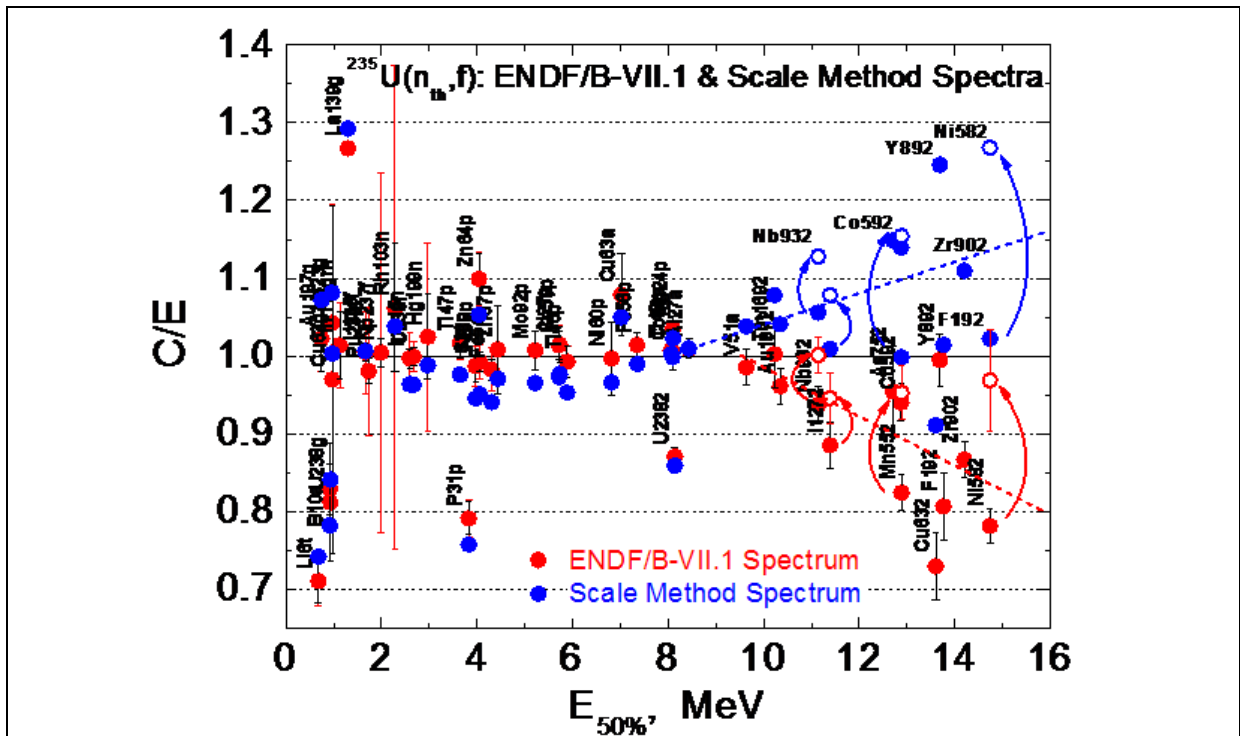


Fig. 2: C/E for the cross sections averaged in the $^{235}\text{U}(n_{\text{th}},f)$ field from ENDF/B-VII.1 and Scale method (N. Kornilov). Uncertainties bars: experimental SPA (black), plus IRDFF-1.03 cross sections (red), PFNS - are excluded. Three curved arrows show the change of C/E for $^{127}\text{I}(n,2n)$, $^{55}\text{Mn}(n,2n)$ and $^{58}\text{Ni}(n,2n)$ when SPA recommended by W. Mannhart are replaced with K. Zolotarev values.

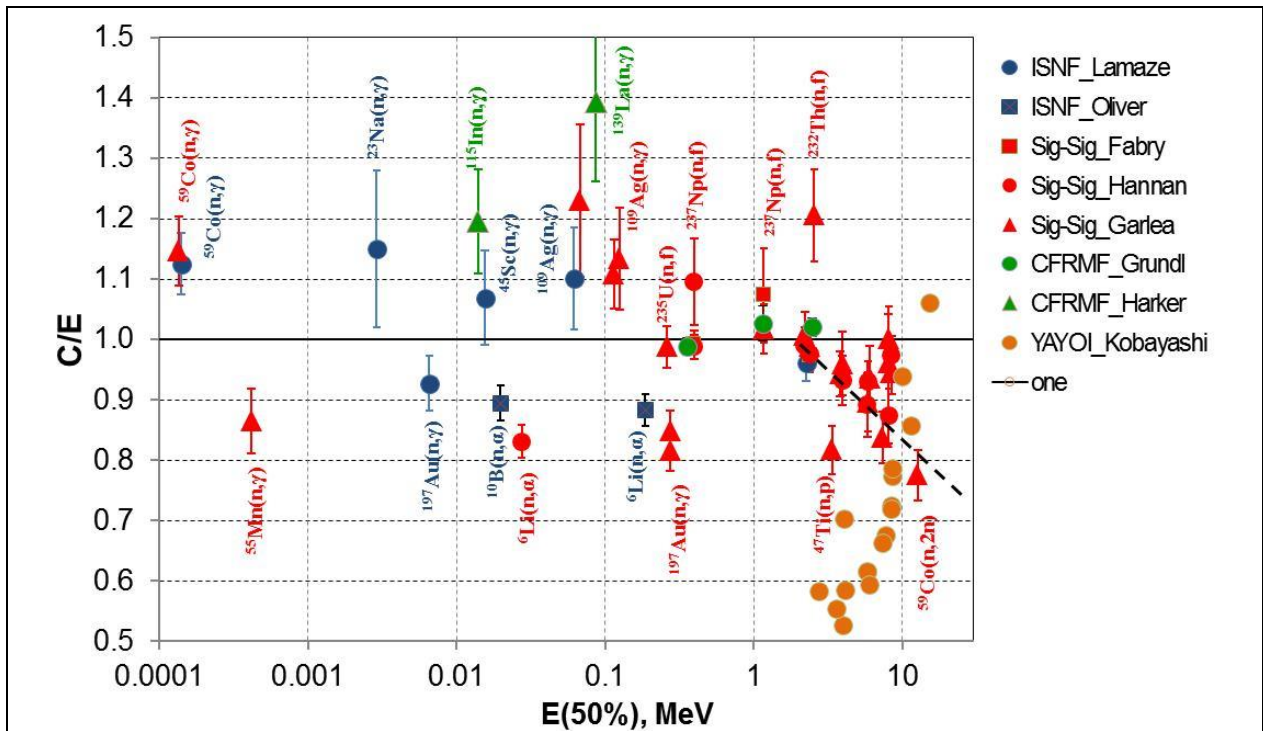


Fig. 3: C/E ratios for SPA in the ISNF, CFRMF, Sigma-Sigma and YAYOI research reactor facilities.

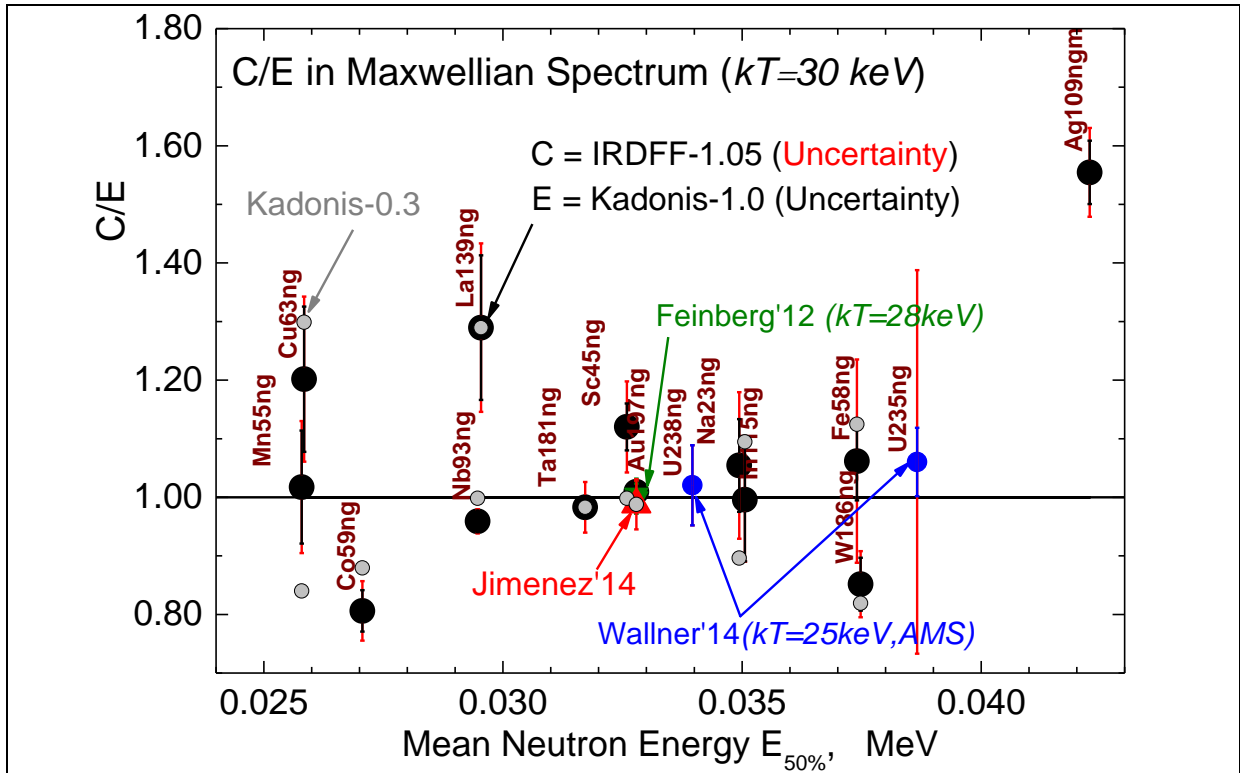


Fig. 4: C/E ratios for SPA in the 30 keV-Maxwellian spectrum. Experimental data: ● - Kadonis-1.0, ○ - Kadonis-0.3, other symbols - EXFOR; calculations – IRDFF-1.05.

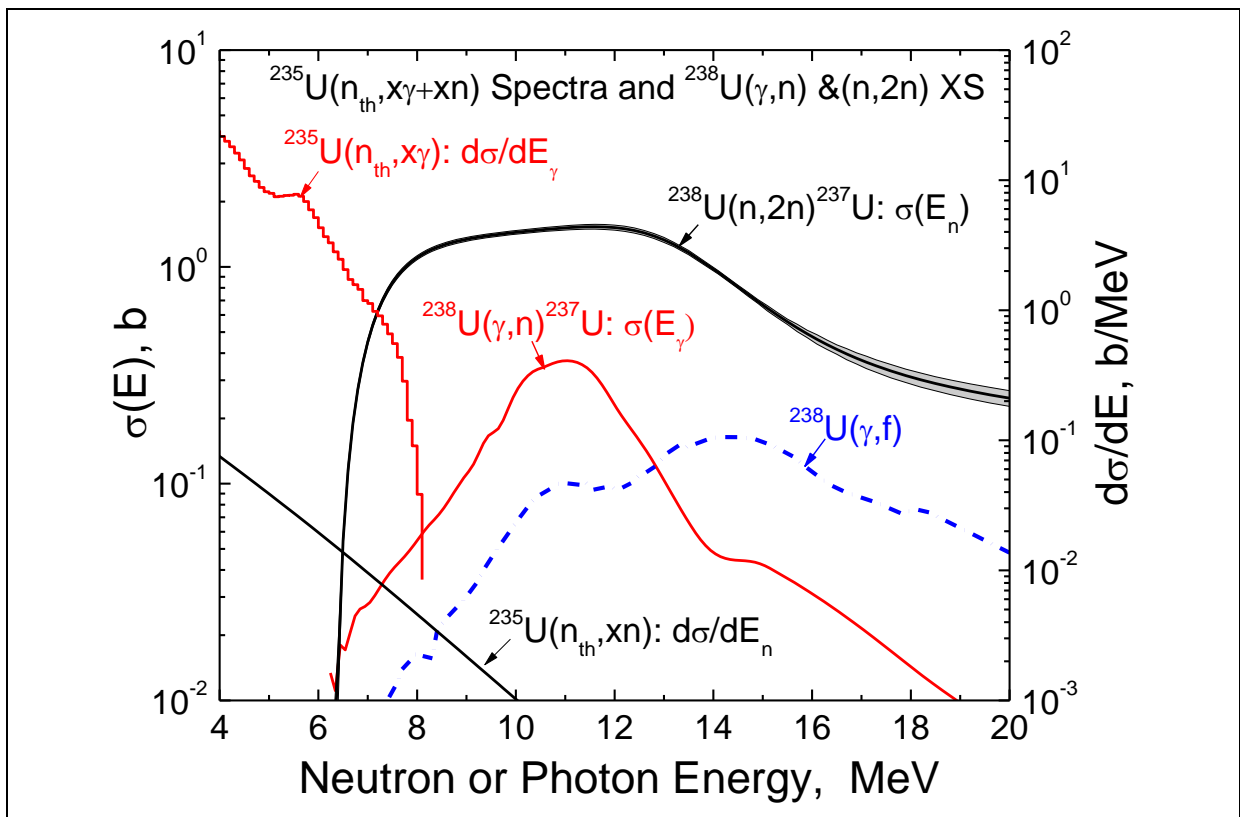


Fig. 5: The $^{235}\text{U}(n_{\text{th}}, X\gamma)$ gamma and $^{235}\text{U}(n_{\text{th}}, xn)$ neutron fields (infinitely thin layer). The cross sections for photonuclear reaction $^{238}\text{U}(\gamma, n)^{237}\text{U}$ from and for neutron dosimetry reaction $^{238}\text{U}(n, 2n)^{237}\text{U}$ from IRDFF-1.05.

The CRP recommends the Atomic Masses, Isotopic Abundancies, neutron induced Fission Yields and Photonuclear cross sections as a supplementary information for IRDFF from following resources:

- Atomic Mass data Evaluation from AME-2002;
- Isotopic Composition of Elements from the Commission on Isotopic Abundances and Atomic Weights CIAAW;
- Neutron induced Fission Yields from the JEFF-3.1.1 library (for IRDFF reactions accessible here Th-232, U-235, U-238, Np-237, Pu-239, Am-241).

The Photo-induced nuclear reactions evaluations are recommended to take from the IAEA Photonuclear Data Library (will be updated in frame of the new IAEA CRP on Photonuclear Data). The (γ,n) process may compete with neutron dosimetry reaction $(n,2n)$, since both produce the same residual isotope. The value of (γ,n) contribution depends on facility and location there since the neutron and gamma fields are produced by neighbouring materials.

For the ideal case, when mixed gamma-neutron field is produced by thermal neutrons in the thin ^{235}U layer and the cross sections are taken from cited photonuclear library and IRDFF-1.05 (as plotted in Fig. 5), the $^{238}\text{U}(\gamma,n)$ reaction contributes about 0.6% to the ^{237}U production by $^{238}\text{U}(n,2n)$. For same case, the $^{23}\text{Na}(\gamma,n)$ reaction does not produce ^{22}Na whereas $^{23}\text{Na}(n,2n)$ does.

A proposal for a new REAL exercise for the international inter-comparison of the modern neutron spectral adjustment codes employing the cross sections from IRDFF was accepted at RCM-2 (March 2015).

Implementing this, the NDS has selected at the moment 13 cases which cover the fission reactors, critical benchmarks, fusion benchmarks and accelerator driven facilities, more information see on the dedicated web-page REAL-201X. The exercise still requires completion of the inputs for several cases, generation of elemental cross sections for the accelerator-driven spectra and testing of cases with one or another adjustment codes.

7.2. Experimental Validation of IRDFF Cross-Sections in Quasi-Monoenergetic Neutron Fluxes in 20-35 MeV Energy Range, M. Majerle, P. Bém, J. Novák, E. Šimečková, M. Štefánik *Nuclear Physics Institute (NPI), Rez, Czech Republic*

The neutron irradiations have been performed with quasi-monoenergetic neutron generator, based on the $p + {}^7\text{Li}$ reaction. The produced neutron spectrum consists of the monoenergetic peak - reaction ${}^7\text{Li}(p,n){}^7\text{Be}(0+0.429\text{keV})$ - and continuous spectrum at energies below the monoenergetic peak, accounting for ca. 50% of the produced neutrons.

Protons were directed at a 2 mm thick lithium foil with a 10 mm carbon backing which fully stopped the protons. The proton beam energies used were 20, 22.5, 25, 27.5, 30, 32.5 and 35 MeV. The width of the monoenergetic peak was determined with the ionization losses of the protons in the lithium foil ranging from 1.5 to 2.5 MeV. The intervals between the proton energies were chosen so that the monoenergetic peaks were slightly overlapping. The energy spread of the proton beam was estimated to have the Gaussian distribution with $\text{FWHM} = 200$ keV, the absolute energy of the protons is defined with the accuracy of 1.5%. The samples were irradiated during about 6 - 10 hours in the target-sample distance 86 mm (flux ca. 10^9 n/cm²/s).

Moreover, additional irradiations using the same type of the neutron generator were performed at The Svedberg Laboratory (TSL) in Uppsala at proton energies 38, 49 and 61 MeV. In their neutron generator the proton beam is not stopped in carbon, but deflected by a magnet into a 10 m long dumping line ending with a heavily shielded water-cooled graphite beam dump. To avoid the contamination of the neutron spectrum with deflected protons, the samples were placed 197 cm from the target front. This resulted in lower neutron flux which was partly compensated with longer irradiation time (about 24 hours for every run).

The irradiated samples were made from high purity (99.9%) metallic Au, Fe, Co, Tm and Bi and had disc shapes with a 15 mm diameter and a thickness ranging from 0.05 mm to 0.5 mm (obtained from Goodfellow). The irradiation intensity was recorded by measuring the proton current at the target assembly and with a stilbene monitor. The beam instabilities were included in the calculation of the reaction rates.

Several radioactive products were detected in the samples using offline γ -spectroscopy employing two calibrated HPGe detectors with 50% efficiency and good energy resolution ($\text{FWHM} = 1.3 - 1.8$ keV). The decay spectra were measured during the cooling period from minutes up to 100 days. The reaction rates of the specific isotopes at the end of the irradiation were calculated using tabulated decay half-lives and gamma-intensities from the ENSDF database. In the frame of this work the intensities of the decay lines of ${}^{196\text{m}2}\text{Au}$ were remeasured and newly obtained values were used in the analysis.

The determination of the neutron spectrum was done in several steps. At NPI, the neutron spectrum was measured using the Time-Of-Flight (TOF) method at a distance of 4-5 m from the target front. The comparison of the measured spectra with the MCNPX simulations showed that MCNPX underestimates the contribution of the neutrons below the monoenergetic peak (factor 1.2-1.6). The absolute number of the neutrons in the monoenergetic peak was obtained from the measured activity of ${}^7\text{Be}$ in the lithium target (offline γ -spectroscopy) and the Uwamino formula for forwardness of the neutron peak. Uwamino measured the angular distribution of peak neutrons on similarly constructed neutron generator (12 mm of carbon instead of 10 mm). The correctness of the absolute number of peak neutrons is already partly (at the moment only the proton energy 32.5 MeV was measured reliably) confirmed by the TOF measurement. Three different 2"x2" NE213 detectors were used for intercomparison of the absolute number of peak neutrons. The results were in agreement up to 1% with the number of neutrons predicted from the number of ${}^7\text{Be}$ nuclei and Uwamino formula. The necessary corrections of the neutron spectrum were introduced at the MCNPX simulated spectra at 86 mm. The determination of the neutron spectra at TSL is in progress. FLUKA simulations (neutron spectrum is implemented in source.f routine) are performed to understand the spectrum, beam homogeneity, neutron scattering and so on. The simulated spectra are compared with TOF measurements using thin oil breakdown counters (TFBC).

The neutron spectra used for the irradiation of the samples consist of the peak neutrons and the continuum. A modified version of the SAND-II code was used to extract the cross-section curves in such complex spectra. The IRDFF v1.05 data were grouped in 0.25 MeV bins and used as the input cross-sections for the SAND-II procedure. After several iterations, the obtained curves are averaged at the regions covered with the monoenergetic peaks to obtain the cross-section.

The width of the monoenergetic peak is used for the uncertainty of the cross-section on the energy scale. The uncertainty on the cross-section scale contains two contributions. The first is the systematic uncertainty at irradiation (repeatability of the reaction rate measurements), which is determined by comparison with previous similar measurements and is below 10%. The reaction rates measured in this work were obtained with better accuracy (mainly because of extra ^7Be activity measurements) and the repeatability is probably better than 5% (to be verified with future measurements). The second contribution originates in the extraction procedure with some uncertainty in neutron spectra and was studied with the sensitivity analysis. The SAND-II extraction procedure was repeated many times (1000 for each parameter) with modified input parameters sampled from normal distribution using their estimated uncertainties. The extracted cross-sections are distributed normally, the uncertainties are determined from the σ/FWHM of this distribution and are up to 10% at highest energies (where the contribution to the reaction rate from uncertain neutron continuum is the highest).

The preliminary results for the (n,xn) on ^{59}Co , ^{169}Tm , ^{209}Bi , ^{54}Fe and ^{197}Au in the energy range 20-35 MeV are obtained. The neutron flux analysis and cross-section determination from the TSL irradiation will be finished in few months. The results will be presented at the NEUDOS-13 conference.

7.3. Analyzing and updating nuclear decay data evaluations to improve the IRDFF Decay sub-library, V. Chechev

Khlopin Radium Institute, St. Petersburg, Russia

The main goal of this research as a part of the *IAEA CRP F41031* [1] is to test, validate and improve the *IRDFF* Decay sub-library. The nuclear decay data of interest for dosimetry applications are radionuclide half-lives, decay modes, energy and intensity of prominent radiation used for the detection of the dosimetry reaction products [2, 3].

The work program has included for radionuclides – dosimetry neutron reaction residuals:

- preliminary analysis of available evaluated decay data containing in the *Evaluated Nuclear Structure Data File (ENSDF)* [4] and also on the *Decay Data Evaluation Project (DDEP)* web site [5],
- testing the evaluated decay data containing in the file *irdf2012.endf* (source on Oct 2012) for validity and determination of the list of radionuclides for which there are available new published experimental data and/or important compilations,
- with using the *DDEP* methodology, analyzing decay schemes and the full re-evaluation/update of decay data for the radionuclides from the above list,
- introducing small update amendments where needed to the existing sets of *NDS/DDEP* evaluated data which mainly retain their validity,

representation of the evaluated decay data for all the considered radionuclides in the *ENSDF* formatting to transfer them into the *ENDF* format.

Detailed information of **implementation of this work program** is given in **Table 1**. The third column produces the dates of evaluations for the file *irdf2012.endf* (source on October 2012). The fourth column gives information of the latest published *NDS* evaluations. The sources and nature of new evaluated decay data for *IRDFF-2017* are presented in the fifth column. Basically, these data are our (V.P. Chechev and N.K. Kuzmenko) special 2015-2017 evaluations for *IRDFF* using *DDEP* methodology and also different existing or corrected *DDEP* evaluations. References to new important experimental data and/or compilations taken into account compared to the evaluations for the file *irdf2012.endf* are listed in the sixth column.

Between the 2nd and 3rd RCM of the CRP F41031 we considered decay data for 52 radionuclides. The evaluated values of their half-lives and prominent gamma ray intensities recommended for use in *IRDFF-2017* are presented in **Table 2**.

Some of the problems associated with the use of new recommended (updated) decay data

One of them is occurrence of strongly discrepant data. The evaluation can give an averaged recommended value with a big uncertainty or select one of the discrepant values. However the best decision in such case is a new additional measurement. An example is the new experimental values of relative gamma-ray intensity in decay of 9,6 h Au-196m₂ from the recent measurement in the Czech Institute of Nuclear Physics by M. Majerle, E. Šimečková, M. Štefánik [6] which was done specifically for the *IRDFF* library because of discrepancy of previously published data. Another problem is related to the influence of new evaluated decay data on determination of dosimetry reaction cross sections which was done previously using old recommended decay data. Relevant amendments to cross sections are significant only in case of great difference of new and previous recommended decay data. The comparison of new values with the previous ones from *IRDFF-2012* is given in **Table 3** for half-lives and prominent gamma-ray intensities in decay of 40 radionuclides.

About problems identified at the 2nd RCM

According actions assigned at the 2nd RCM nuclear decay data problems were examined for the following nuclides:

- Rh-103m - x-ray emission probability around 20 keV;
- La-140 - gamma intensities for lines below 1596 keV;
- W-187 - gamma intensities of 2 lines (473.53 keV and 685.81 keV);
- Cu-64 - 511 keV annihilation gamma line intensity tends to be increased essentially.

Conclusion

As a result, at present there are available modern evaluated decay data for 72 radionuclides - dosimetry neutron reaction residuals of 102 ones listed on the *IRDF* web site. Of 30 remaining, relatively recent 2009-2013 *NDS* publications are available for 28 nuclides. Only for Nb-94m and Au-194 updating is required.

Proposed activities in the frame of CRP for 2017:

- analysing decay schemes and updating decay characteristics for Nb-94m and Au-194
 - correcting some decay data evaluated for *IRDF* library in 2014 and 2015
- testing the 2009-2013 *NDS* decay data publications for 28 radionuclides

References

1. The IAEA CRP F41031 “Testing and Improving the IAEA International Dosimetry Library for Fission and Fusion (IRDF)”: <https://www-nds.iaea.org/IRDFtest/>.
2. Summary Report of the 2nd RCM CRP F41031. Prepared by P.J. Griffin, L.R. Greenwood, S.P. Simakov. – INDC(NDS)-0682, IAEA, Vienna, March 2015.
3. List of Isotopes and Isomers produced by reactions included in IRDF. URL: <https://www-nds.iaea.org/IRDFtest/irdffnuclideslist.htm>
4. Evaluated Nuclear Structure Data File (ENSDF). New York: Brookhaven National Laboratory. URL: <http://www.nndc.bnl.gov/ensdf/>
5. Recommended Data by the Decay Data Evaluation Project working group. URL: http://www.nucleide.org/DDEP_WG/DDEPdata.htm
6. M. Majerle, E. Šimečková, M. Štefánik. *Intensities of the gamma lines from the decay of $^{196m2}\text{Au}$* . Private Communication, Nuclear Physics Institute of ASCR PRI, 250 68 Řež, Czech Republic, 2015.

7.4. Advanced UQ Approaches to the Validation of Dosimetry Cross Sections in Reactor Benchmark Fields: Input to 3rd RCM, P. Griffin

¹*Sandia National Laboratories1, Radiation and Electrical Sciences Center, Albuquerque, NM, 87185-1146, USA*

Executive Summary. This report summarizes the progress made by Sandia National Laboratories in its support of the International Atomic Energy Agency (IAEA) Nuclear Data Section (NDS) Cooperative Research Project (CRP) on the testing and improving of the International Reactor Dosimetry and Fusion File (IRDF). We have surveyed a set of applicable UQ approaches for the analysis of the consistency of integral cross section measurements in neutron benchmark fields. The conclusion was that, for reactor fields, the best approach was a least-squares methodology that addressed the combined uncertainty from the neutron spectrum, i.e. the uncertainty from the characterization the neutron spectrum in the benchmark field, the measured activity for the dosimetry reaction, and the dosimetry cross section for which validation evidence was being sought. This least square approach was then applied to the ²⁵²Cf spontaneous fission standard benchmark field, the ²³⁵U thermal fission reference benchmark field, and to seven different reactor-based reference benchmark neutron fields ranging from a highly enriched ²³⁵U fast burst metal assembly to a well-moderated pool-type reactor field. This validation effort provided good validation evidence for 64 of the IRDF reactions. The ²⁵²Cf(sf) field provided validation evidence for 46 reactions. The ²³⁵U(th) field provided validation evidence for 50 reactions, 8 of which had not been validated in the ²⁵²Cf(sf) standard benchmark field. The analysis of the reactor field included sensors fielded with covers that shifted the energy range for the response of the dosimeters. When the best validation data gathered from these seven reactor fields were considered, reactor-based validation evidence existed for 40 reactions, 10 of which had not been validated in either the ²⁵²Cf(sf) or ²³⁵U(th) neutron fields. We concluded the effort by identifying efforts that should be pursued in reactors that could further enhance the validation of the IRDF dosimetry library and the reactions where the community needs to look to accelerator-produced neutron fields for validation evidence.

Survey of Dosimetry Metrics

This is the report from Sandia National Laboratories (SNL), presented at the 3rd Research Coordination Meeting (RCM) on Testing and Improving the IAEA International Reactor Dosimetry and Fusion File (IRDF) Cooperative Research Project (CRP), on our recent progress in this project [1]. It is clear that all validation data must be accompanied by a quantitative statement on the uncertainty between a measured and a calculated quantity. One of the critical aspects of our research has been an examination of the relative merits of various metrics that can be used to report the validation results. The relative merits of a validation approach can differ with the selection of the measurement data to be addressed in the validation activity and in sources of uncertainty that are applicable to those measurements. Since differential cross section data, e.g. monoenergetic neutron cross section measurements, were considered in the preparation of the evaluated cross sections, data from these measurements cannot be used to assert an independent validation of the cross sections. Thus, for validation evidence, we looked primarily to comparisons with integral measurements obtained in benchmark neutron fields. One of our first activities was to explore various validation metrics and to compare the strength of the validation evidence that they could provide when applied to existing data in the neutron benchmark fields.

Commonly used validation metrics include use of a calculated-to-experimental (C/E) ratio for: a) a spectrum-averaged cross section; b) a spectral index; or c) use of a constrained least squares fit to activation data while reporting a chi-squared per degree of freedom (dof) for each measured activity. Each metric has its advantages and disadvantages. The relevant input data used in a numerical quantification of the validation metric (and its associated uncertainty) include the energy-dependent reaction cross sections, activity measurements, benchmark field neutron source spectrum, and nuclear decay data (half-life, gamma emission rates). One must also take into consideration correlations in the

¹ Sandia is a multi-mission laboratory operated by Sandia Corporation, a Lockheed Martin Company, for the United States Department of Energy under contract DE-AC04-94AL85000.

input data and properly propagate all uncertainty contributions. A discussion of the pros and cons of these various validation metrics in various benchmark fields has been captured in references 2 and 3. While approach a) has great benefit in the very well characterized ^{252}Cf spontaneous fission standard benchmark field [4], when one considers the larger spectrum uncertainties associated with the spectrum characterization in the ^{235}U thermal fission reference benchmark neutron field, the common approach has been to go over to the option b) validation metric of the spectral index. The problem here is that only a sparse set of validation data is available for spectral indices [5]. The use of option c), a constrained least squares consideration of a set of measurements, addresses the large uncertainty in the $^{235}\text{U}(\text{th})$ neutron spectrum and also resolves the lack of spectral index measurement data in the $^{235}\text{U}(\text{th})$ field. When one considers validation data gathered in reactor-based reference benchmark neutron fields, option c) is the most viable approach [2,3].

Application of the Least Squares Dosimetry Metrics to Reactor-Based Neutron Benchmark Fields

In addition to the $^{252}\text{Cf}(\text{sf})$ and $^{235}\text{U}(\text{th})$ neutron benchmark fields, other well-characterized reference neutron benchmark fields that can contribute to the body of validation evidence for the IRDFF dosimetry cross sections and were considered in our work include the following seven reactor fields:

- Sandia Pulsed Reactor (SPR-III), a fast burst reactor (FBR) cavity (SPR-III-CC)
- 6-inch leakage in a tripod configuration around a fast burst reactor (Tripod-FF-L-6-cl)
- central cavity of the Annular Core Research Reactor (ACRR), an under-moderated pool-type reactor (ACRR-FF-CC-32-cl)
- $\text{Pb-B}_4\text{C}$ bucket in the ACRR cavity, a filtered high energy neutron spectrum with low gamma environment (ACRR-LB44-32-CL)
- polyethylene-lead-graphite (PLG) bucket in the ACRR cavity, a moderated pool-type neutron reactor environment (ACRR-PLG-CC-32-cl)
- Cd-polyethylene bucket in the ACRR central cavity, a more moderated and high gamma environment (ACRR-CdPoly-CC-32-cl)
- fueled external cavity (FREC-II) coupled with the ACRR, a large volume exposure configuration with minimal fluence gradient (ACRR-FRECII-FF-cl)
- Figure 1 compares the differential energy neutron spectrum for four of these fields with that from the standard ^{252}Cf standard benchmark field. Figure 2 shows the C/E ratio for some of the activity measurements gathered in these reactor fields.

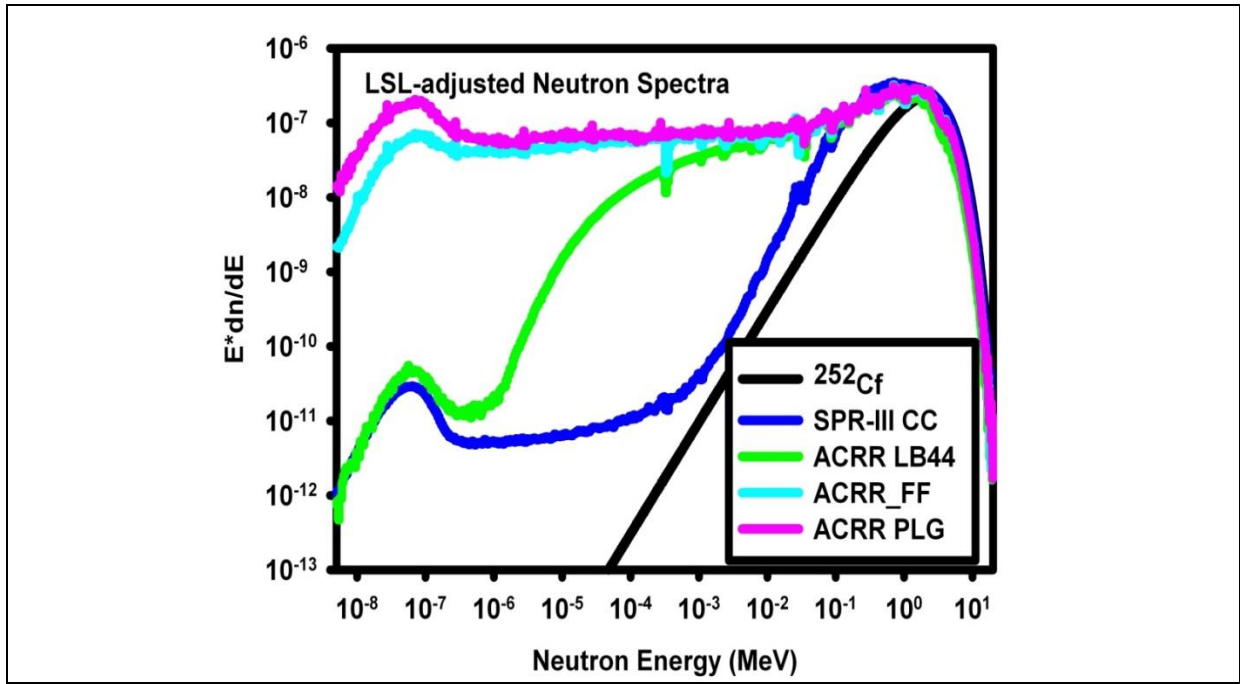


Fig. 1: Representative Neutron Spectrum in Benchmark Fields

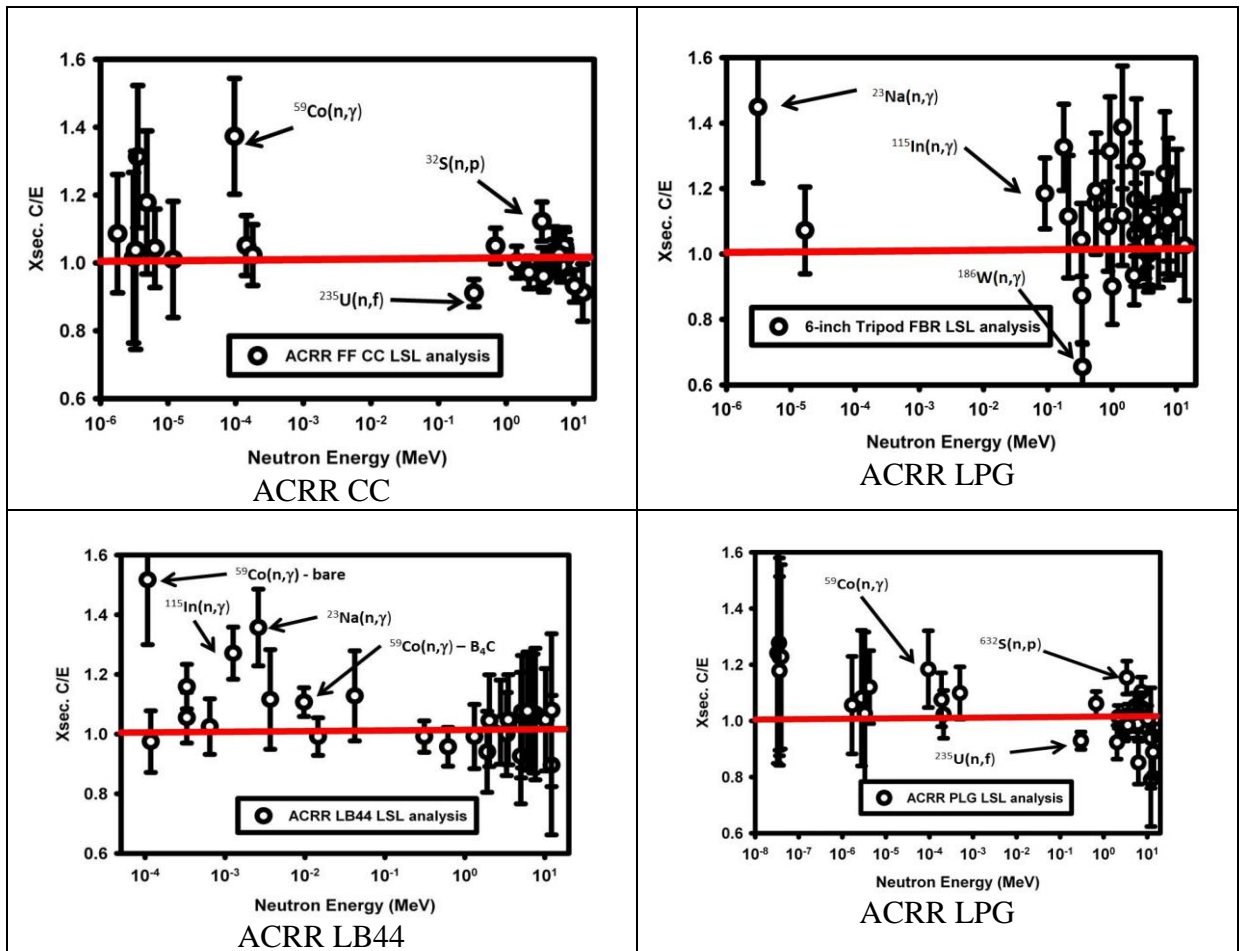


Fig. 2: C/E Ratio for Least Square Constrained Activity Ratio for Important

Dosimetry Reactions in Reactor-based Neutron Benchmark Fields Results of Least Squares Analysis as the Validation Metric

Table 1 shows the number of dosimetry-relevant activity measurements were available for each of the seven reactor-based benchmark fields. These calculated-to-experimental (C/E) ratios were analyzed using the SNL-LSL least squares code and the version 1.05 of the IRDFF cross sections. This table also shows the initial chi-squared per degree of freedom (dof), χ^2/dof , when all of the available data was used in the least square analysis.

Table 1: Summary of Reactor-based Validation Evidence

| Reactor Environment | Number of “Foil/Cover” Combinations Measured | Initial χ^2/dof | Number of validated Dosimetry reactions |
|-----------------------|--|-----------------------------|---|
| SPR-II CC | 42 | 2.91 | 31 [4] |
| ACRR CC | 35 | 0.9883 | 27 [1] |
| ACRR LB44 | 33 | 1.945 | 27 [0] |
| ACRR PLG | 37 | 1.095 | 29 [0] |
| ACRR Cd-Poly | 33 | 1.810 | 31 [0] |
| 6” Tripod FBR Leakage | 31 | 2.281 | 24 [0] |
| ACRR FREC-II | 33 | 1.701 | 30 [0] |

In evaluating validation evidence, one needs to have a clear set of criteria of what constitutes acceptable behaviour in the analysis of the dataset. Table 2 shows the criteria that were considered in making this decision for the reactor-based least square C/E analysis. Note, one figure of merit was not considered sufficient to constitute a decision that the cross section validation evidence was acceptable. Criteria were placed on the number of standard deviations that the C/E could deviate from the nominal value of unity for that activity measurement of the given dosimetry reaction, for the overall value of the C/E metric, and for the magnitude of the uncertainty associated with the experimental activity measurement. The green/orange/red shading is used in the table to distinguish good/acceptable/poor performance based on each of the criteria. A discrepant behavior in any of these criteria in the least squares analysis cast doubt on the acceptability of the validation evidence.

The last column in Table 2 indicates the number of validated reactions that came from the inspection of the measurements gathered in this field and used in the least square analysis. Note, in this work covers were used on many of the dosimetry foils that were fielded. The covers were often Cadmium or a combination of Cadmium inside a larger enriched $^{10}\text{B}_4\text{C}$ ball. Details on how the cover correction to the response of the dosimetry reaction was treated can be found in Reference 7. Details on the derivation of the *a priori* covariance matrix for the neutron spectrum used in the least square spectrum adjustment can be found in Reference 8. This use of various covers meant that different C/E metrics were produced for the different cover/reaction combinations. In the last column of Table 2 the number of validated reactions in this field are indicated. This number does not count as distinct data gathered from the different cover/reaction combinations. This deliberate avoidance of double counting a reaction for validation evidence with difference covers is the reason that the number of validated ‘reactions’ in column 4 can be significantly larger than the number of “foil/cover” combinations indicated in column 2. The decision on what constituted “acceptable” validation evidence was made based on the body of C/E data gathered for the dosimeters that were fielded in that spectral characterization, i.e. all cover combinations. The number appearing in the square brackets in column 4, after the number of validated reactions, indicates the number of validated reactions in that field that had not been validated in any of the “previous” benchmark fields. By “previous” we mean not in the $^{252}\text{Cf}(\text{sf})$ standard benchmark field, nor in the $^{235}\text{U}(\text{th})$ reference benchmark field, nor in the reactor-based reference benchmark fields appearing in higher rows in the table.

Table 2: Criteria Used to Evaluate Consistency Validation Evidence Based on a Least Square Adjustment Analysis for Various Reactions

| # | Metric | Status | | |
|---|--------------|-------------------|--------------------|---------------------|
| | | Good | Acceptable | Poor |
| 1 | C/E | < 2 std. dev. | < 3 std. dev. | > 3 std. dev. |
| 2 | C/E interval | Within [0.9, 1.1] | Within [0.8, 1.25] | Outside [0.8, 1.25] |
| 3 | Expt. Unc. | < 15% | < 50% | > 50% |

IRDF Validation Status Based on this Work

The above analysis shows that application of the least squares approach to supplying validation evidence provides validation evidence for 64 of the IRDF version 1.05 dosimetry cross sections. Validation evidence for 46 of these reactions came from the analysis of data gathered in the $^{252}\text{Cf}(\text{sf})$ reference benchmark field. Validation evidence for an additional 8 reactions came from the least square analysis of the data in the $^{235}\text{U}(\text{th})$ reference benchmark field. Data for another 10 reactions came from consideration of the seven reactor-based reference benchmark fields. Table 3 provides a summary of the validation evidence from the various benchmark fields. The value of the C/E along with the uncertainty obtained from the constrained least square analysis in that field appears in the various columns. The last column, containing the reactor-based validation evidence, shows the C/E evidence for the “best” baseline reactor environment investigated. Note, in this consideration of “best”, preference was given for dosimetry evidence gathered with the “bare” foil.

In Table 3 the “Reaction Label” column is shaded to indicate the overall status of the validation of that reaction. An unshaded reaction identifier indicates a reaction where no validation evidence was considered for that reaction. A “yellow” shading is given to a dosimetry-relevant reaction that was not found in the IRDF version 1.05 library or not relevant when considering the issue of validated reactions. The “yellow” shading is applied to “redundant” reactions, such as the $^{\text{nat}}\text{Ti}(\text{n},\text{X})^{47}\text{Sc}$ reaction where the status of the validation evidence is indicated by a combined examination of the $^{47}\text{Ti}(\text{n},\text{p})^{47}\text{Sc}$ and $^{48}\text{Ti}(\text{n},\text{np};\text{d})^{47}\text{Sc}$ reactions. The “yellow” status for the $^{32}\text{S}(\text{n},\text{p})\text{-Cf-Eqv.}$ reaction is because it represents a transfer calibration for the $^{32}\text{S}(\text{n},\text{p})^{32}\text{P}$ reaction using an exposure in the $^{252}\text{Cf}(\text{sf})$ field. These yellow shadings can also be seen for some interferent/impurity reactions that should be considered when evaluating the validation evidence in some neutron fields, e.g. the $^{11}\text{B}(\text{n},\alpha)^8\text{Li}$ reaction. A “yellow” shading is also used for special responses to fission foils where the contributions from other fissionable impurities in the foil could play a role and have been taken into account in the analysis, e.g. SNLPU, SNLEU and SNLDU reactions.

We note that the least square analysis only considered the neutron energy range up to 20 MeV. Thus, reactions that had a threshold above 20-MeV could not have been considered in this analysis even if experimental data had been available. Code modifications to the SNL-LSL code will need to be made before this analysis can be used to consider analysis of reactions in neutron fields where a significant portion of the response comes from higher energies. An alternative approach is to use the latest version of the STAYSL code for the spectrum adjustment since it has been modified to use the IRDF library and to treat energies up to 60 MeV.

We note that Table 3 does not show any “red” discrepant reactions. There are some “discrepant” entries for various neutron fields that should be investigated in more detail, but no reaction was found to be discrepant in all of the fields investigated. There were several “orange” reactions where validation data was available but where it needed to be augmented with improved measurements.

Table 3: C/E for Activity Measurements in Neutron Benchmark Fields Based on Least Square Spectrum Adjustment

| ID # | Reaction Label | Baseline C/E | | Supplemental C/E |
|------|---|-----------------------|----------------------|---|
| | | ²⁵² Cf(sf) | ²³⁵ U(th) | Best Bare Rx from Composite of Reactor Fields |
| 1 | ⁶ Li(n,t) ⁴ He | --- | 1.040±4.103% | --- |
| 2 | ⁶ Li(n,nd:2np) ⁴ He | --- | --- | --- |
| 3 | ⁷ Li(n,2nα) ² H | --- | --- | --- |
| 4 | ⁷ Li(n,3nα) ¹ H | --- | --- | --- |
| 7 | ¹⁰ B(n,α) ⁷ Li | --- | 1.3033±4.128% | --- |
| 8 | ¹⁰ B(n,t)2α | --- | --- | --- |
| 9 | ¹⁰ B(n,X) ⁴ He | --- | --- | --- |
| 11 | ¹¹ B(n,α) ⁸ Li | --- | --- | --- |
| 12 | ¹¹ B(n,nα) ⁷ Li | --- | --- | --- |
| 13 | ¹¹ B(n,X) ⁴ He | redundant | redundant | --- |
| 15 | ^{nat} B(n,X) ⁴ He | redundant | redundant | --- |
| 20 | ¹⁹ F(n,2n) ¹⁸ F | 1.000±5.646% | 0.8257±11.75% | --- |
| 21 | ²³ Na(n,2n) ²² Na | ---- | --- | --- |
| 22 | ²³ Na(n,γ) ²⁴ Na | 0.8050±13.65% | --- | 1.043±11.09% |
| 23 | ²⁴ Mg(n,p) ²⁴ Na | 1.048±2.916% | 1.007±4.697% | 1.041±4.976% |
| 24 | ²⁷ Al(n,α) ²⁴ Na | 0.9956±2.193% | 1.011±4.481% | 1.078±14.90% |
| 25 | ²⁷ Al(n,p) ²⁷ Mg | 0.9463±1.959% | 0.9715±3.147% | 0.9618±4.412% |
| 26 | ²⁸ Si(n,p) ²⁸ Al | 0.9939±3.763% | 1.000±4.91% | --- |
| 27 | ²⁹ Si(n,d:np) ²⁸ Al | --- | --- | --- |
| 29 | ³¹ P(n,p) ³¹ Si | 0.8629±10.45% | 0.8716±5.078% | --- |
| 30 | ³² S(n,p) ³² P | 1.016±3.654% | 0.9969±2.502% | 1.106±11.50% |
| --- | ³² S(n,p)-Cf-Eqv. | redundant | redundant | 1.045±5.113% |
| 33 | ⁴⁵ Sc(n,γ) ⁴⁶ Sc | --- | --- | 1.022±16.65% |
| 34 | ⁴⁶ Ti(n,p) ⁴⁶ Sc | 0.9687±2.582% | 0.9921±3.405% | 1.021±4.738% |
| 35 | ⁴⁶ Ti(n,2n) ⁴⁵ Ti | 1.992±33.99% | --- | --- |
| 36 | ⁴⁷ Ti(n,p) ⁴⁷ Sc | 1.009±2.161% | 1.030±2.629% | 0.9744±4.705% |
| 37 | ⁴⁷ Ti(n,np:d) ⁴⁸ Sc | --- | --- | --- |
| 39 | ⁴⁸ Ti(n,p) ⁴⁸ Sc | 0.9993±3.527% | 1.009±5.143% | 1.038±5.075% |
| 40 | ⁴⁸ Ti(n,np:d) ⁴⁷ Sc | --- | --- | --- |
| 41 | ⁴⁹ Ti(n,np:d) ⁴⁸ Sc | --- | --- | --- |
| 42 | ^{nat} Ti(n,X) ⁴⁶ Sc | redundant | redundant | redundant |
| 43 | ^{nat} Ti(n,X) ⁴⁷ Sc | redundant | redundant | redundant |
| 44 | ^{nat} Ti(n,X) ⁴⁸ Sc | redundant | redundant | redundant |
| 45 | ⁵¹ V(n,α) ⁴⁸ Sc | 0.9827±3.230% | 0.9908±5.748% | --- |
| 46 | ⁵² Cr(n,2n) ⁵¹ Cr | --- | --- | --- |
| 47 | ⁵⁵ Mn(n,γ) ⁵⁶ Mn | --- | --- | 0.9847±8.685% |
| 48 | ⁵⁵ Mn(n,2n) ⁵⁴ Mn | 1.015±4.101% | 0.9802±10.24% | 0.9492±9.832% |
| 49 | ⁵⁴ Fe(n,2n) ⁵³ Fe | --- | --- | --- |
| 50 | ⁵⁴ Fe(n,α) ⁵¹ Cr | --- | 0.9913±7.377% | --- |
| 51 | ⁵⁴ Fe(n,p) ⁵⁴ Mn | 1.009±1.786% | 1.016±2.118% | 1.014±4.507% |
| 52 | ⁵⁶ Fe(n,p) ⁵⁶ Mn | 0.9919±2.913% | 1.009±4.305% | 1.004±4.733% |
| 54 | ⁵⁸ Fe(n,γ) ⁵⁹ Fe | --- | --- | 0.9813±9.196% |
| 56 | ⁵⁹ Co(n,p) ⁵⁹ Fe | 1.009±3.162% | 1.019±3.728% | 1.001±5.176% |

| | | | | |
|-----|--|---------------|---------------|---------------|
| 57 | $^{59}\text{Co}(n,\gamma)^{60}\text{Co}$ | 0.6970±6.412% | --- | 0.8926±28.26% |
| 58 | $^{59}\text{Co}(n,2n)^{58}\text{Co}$ | 1.001±4.271% | 0.9680±9.940% | 1.090±16.6% |
| --- | $^{59}\text{Co}(n,3n)^{57}\text{Co}$ | | | --- |
| 59 | $^{59}\text{Co}(n,\alpha)^{56}\text{Mn}$ | 0.9939±2.887% | 1.000±5.275% | 0.4603±14.95% |
| 60 | $^{58}\text{Ni}(n,2n)^{57}\text{Ni}$ | 0.9482±6.912% | 0.8066±14.59% | 1.014±16.69% |
| 61 | $^{58}\text{Ni}(n,p)^{58}\text{Co}$ | 0.9950±1.657% | 1.000±2.007% | 1.000±4.471% |
| 63 | $^{60}\text{Ni}(n,p)^{60}\text{Co}$ | 1.166±5.67% | 0.9970±5.728% | 1.025±6.624% |
| 64 | $^{63}\text{Cu}(n,2n)^{62}\text{Cu}$ | 1.032±5.736% | 0.7249±12.21% | --- |
| 65 | $^{63}\text{Cu}(n,\gamma)^{64}\text{Cu}$ | 0.9909±8.578% | 1.138±17.01% | 1.025±9.085% |
| 66 | $^{63}\text{Cu}(n,\alpha)^{60}\text{Co}$ | 0.9997±2.880% | 1.076±6.089% | 0.9668±13.97% |
| 67 | $^{65}\text{Cu}(n,2n)^{64}\text{Cu}$ | 0.9870±3.712% | --- | --- |
| 68 | $^{64}\text{Zn}(n,p)^{64}\text{Cu}$ | 1.003±2.430% | 1.370±3.38% | 0.9848±4.695% |
| | $^{67}\text{Zn}(n,p)^{67}\text{Cu}$ | --- | 1.017±3.816% | --- |
| 71 | $^{75}\text{As}(n,2n)^{74}\text{As}$ | --- | 0.9818±11.51% | --- |
| 72 | $^{89}\text{Y}(n,2n)^{88}\text{Y}$ | --- | 1.023±11.63% | --- |
| 73 | $^{90}\text{Zr}(n,2n)^{89}\text{Zr}$ | 0.9761±5.773% | 0.8933±12.88% | 1.026±16.38% |
| 77 | $^{93}\text{Nb}(n,\gamma)^{94}\text{Nb}$ | --- | --- | 0.7097±14.74% |
| 78 | $^{93}\text{Nb}(n,2n)^{92\text{m}}\text{Nb}$ | 0.9936±4.987% | 1.025±8.051% | 1.005±4.848% |
| 79 | $^{93}\text{Nb}(n,n')^{93\text{m}}\text{Nb}$ | 1.002±3.345% | 0.9700±8.812% | --- |
| 82 | $^{92}\text{Mo}(n,p)^{92\text{m}}\text{Nb}$ | 0.5162±4.960% | 1.012±3.942% | --- |
| 83 | $^{98}\text{Mo}(n,\gamma)^{99}\text{Mo}$ | --- | --- | 1.009±12.40% |
| 87 | $^{103}\text{Rh}(n,n')^{103\text{m}}\text{Rh}$ | 1.154±10.91% | 0.9995±5.578% | --- |
| 88 | $^{109}\text{Ag}(n,\gamma)^{110\text{m}}\text{Ag}$ | --- | --- | 1.051±18.07% |
| 90 | $^{113}\text{In}(n,\gamma)^{114\text{m}}\text{In}$ | --- | --- | --- |
| 91 | $^{113}\text{In}(n,n')^{113\text{m}}\text{In}$ | 0.9720±2.056% | 0.9390±5.204% | --- |
| 92 | $^{115}\text{In}(n,\gamma)^{116\text{m}}\text{In}$ | 0.9714±2.449% | 0.9353±4.148% | 1.185±9.166% |
| 93 | $^{115}\text{In}(n,n')^{115\text{m}}\text{In}$ | 0.9591±1.568% | 1.009±1.556% | 0.9609±6.494% |
| 94 | $^{115}\text{In}(n,2n)^{114\text{m}}\text{In}$ | --- | --- | --- |
| 95 | $^{127}\text{I}(n,2n)^{126}\text{I}$ | 1.012±3.873% | 0.9704±8.789% | --- |
| 101 | $^{139}\text{La}(n,\gamma)^{140}\text{La}$ | | 1.282±25.22% | --- |
| 104 | $^{141}\text{Pr}(n,2n)^{140}\text{Pr}$ | --- | --- | --- |
| 107 | $^{169}\text{Tm}(n,2n)^{168}\text{Tm}$ | 0.9758±6.656% | 1.016±7.847% | --- |
| --- | $^{169}\text{Tm}(n,3n)^{168}\text{Tm}$ | | | --- |
| 108 | $^{181}\text{Ta}(n,\gamma)^{182\text{m}}\text{Ta}$ | 0.9314±5.607% | --- | --- |
| 109 | $^{186}\text{W}(n,\gamma)^{187}\text{W}$ | --- | --- | 1.010±16.97% |
| 110 | $^{197}\text{Au}(n,\gamma)^{198}\text{Au}$ | 0.9683±1.768% | 0.8545±5.352% | 0.9746±10.59% |
| 111 | $^{197}\text{Au}(n,p)^{197}\text{Pt}$ | | | --- |
| 112 | $^{197}\text{Au}(n,2n)^{196}\text{Au}$ | 0.9985±2.852% | 0.9753±6.962% | --- |
| 113 | $^{197}\text{Au}(n,3n)^{195}\text{Au}$ | --- | --- | --- |
| 115 | $^{199}\text{Hg}(n,n')^{199\text{m}}\text{Hg}$ | 0.9793±2.211% | 1.033±5.909% | --- |
| 116 | $^{204}\text{Pb}(n,n')^{204\text{m}}\text{Pb}$ | 0.9488±1.991% | 0.9189±8.455% | --- |
| --- | $^{209}\text{Bi}(n,3n)^{207}\text{Bi}$ | --- | --- | --- |
| 117 | $^{232}\text{Th}(n,\gamma)^{233}\text{Th}$ | 0.9953±6.929% | --- | --- |
| 118 | $^{232}\text{Th}(n,2n)^{231}\text{Th}$ | --- | --- | --- |
| 119 | $^{232}\text{Th}(n,f)\text{FP}$ | 0.8807±3.160% | 0.9266±3.306% | --- |
| 121 | $^{235}\text{U}(n,f)\text{FP}$ | 1.007±1.208% | 1.017±1.230% | 1.046±6.207% |
| --- | $^{235}\text{U}(n,\gamma)^{236}\text{U}$ | --- | --- | --- |
| 129 | SNLEU | --- | --- | 1.084±12.60% |
| 122 | $^{238}\text{U}(n,f)\text{FP}$ | 0.9724±1.699% | 1.013±1.352% | 1.047±10.37% |

| | | | | |
|-----|---|---------------|---------------|---------------|
| 130 | SNLDU | --- | --- | 1.167±14.87% |
| --- | ²³⁸ U(n, γ) ²³⁹ U | | | --- |
| --- | ²³⁸ U(n,2n) ²³⁷ U | --- | 0.8097±10.87% | --- |
| 123 | ²³⁷ Np(n,f)FP | 0.9939±1.608% | 1.018±1.930% | 1.116±13.54% |
| 124 | ²³⁹ Pu(n,f)FP | 0.9861±1.379% | 0.9932±1.727% | 1.115±6.215% |
| 131 | SNLPU | --- | --- | 0.9007±12.88% |
| 125 | ²⁴⁰ Pu(n,f)FP | --- | --- | --- |
| 126 | ²⁴¹ Pu(n,f)FP | --- | --- | --- |
| 127 | ²⁴² Pu(n,f)FP | --- | --- | --- |
| 128 | ²⁴¹ Am(n,f)FP | --- | --- | --- |

Conclusions

The usefulness of several validation metrics has been investigated and the value of the metrics demonstrated by applying them to the ²³⁵U thermal fission, ²⁵²Cf spontaneous fission, and to various reactor reference fields for which there exists a good database of measured dosimetry cross sections. A coupled least square analysis that includes the cross section along with the spectral representation and the measurements appears to be the most useful validation metric. The validation evidence using this least squares C/E metric has been summarized and reactions have been identified that are in need of additional validation evidence.

References

1. International Reactor Dosimetry and Fusion File, IRDFF v.1.05, October 9, 2014, see <https://www-nds.iaea.org/IRDFF/>
2. P.J. Griffin, E.J. Parma, D.W. Vehar, “Advanced UQ Approaches to the Validation of the IRDFF Library”, Physics of Reactors 2016 (PHYSOR 2016): Unifying Theory and Experiments in the 21st Century, American Nuclear Society, pp. 347 – 361, 2016.
3. P. J. Griffin, “Use of Neutron Benchmark Fields for the Validation of Dosimetry Cross Sections,” European Physical Journal, 2015, presented at ISRD15.
4. S. Simakov, R. Capote, L. Greenwood, P. Griffin, V. Pronyaev, A. Trkov, K. Zolotarev, “Validation of IRDFF in ²⁵²Cf standard and IRDF-2002 reference neutron fields”, European Physical Journal, 2015, presented at ISRD15.
5. J.A. Grundl, C.M. Eisenhauer, NBSIR 85-03151, *Compendium of Benchmark Neutron Fields for Reactor Dosimetry*, US Department of Commerce, National Bureau of Standards, January 1986.
6. P.J. Griffin, “Covariance Propagation in Spectral Indices”, *Nuclear Data Sheets*, **123**, pp. 104 - 108, URL <http://www.sciencedirect.com/science/article/pii/S0090375214006978> (2015).
7. P.J. Griffin, “A rigorous treatment of self-shielding and covers in neutron spectra determinations”, IEEE TNS, pp. 1878-1885, Vol. 42, 1995.
8. Williams, J. G. and Griffin, P. J., Physically Constrained Adjustment of Calculated Neutron Spectra for Dosimetry and Vessel Locations, *Reactor Dosimetry: Radiation Metrology and Assessment* ASTM STP 1398, pp. 494-501, 2001.

7.5. Benchmarking of IRDFF Against 14 MeV Neutron Experiments, M. Angelone

Division of Fusion Centro Ricerche Energia, Frascati, Italy

ENEA activities on IRDFF testing and validation is mainly focussed at validating the IRDFF file at neutron fusion relevant energy (14 MeV). ENEA is mainly using the IRDFF file in substitution of the old IRDF-2002 file for dosimetry calculation (reaction rates) in nuclear analysis of tokamak and in fusion neutronics benchmark and mock-up experiments.

To this end, the previous ENEA effort was devoted to the re-analysis of two benchmark experiments performed at the Frascati neutron generator (FNG). The reaction rates (RR) of the measured activation reactions were re-calculated with the IRDFF_v1.05 file and compared to the results previously obtained with IRDF-2002 file. A second part of the effort was devoted to perform a dedicated experiment at FNG in which activation foils characterized by high threshold reactions (Nb, Al, Ni, In, Zr, Au) were irradiated at various angles around the FNG target (i.e. different neutron energies around 14 MeV). The measured RR were compared to the calculated ones using the MCNP5 code, FENDL-3 transport library and IRDFF_v1.05 dosimetry file. The results were compared to the results obtained using IRDF-2002.

The output of the above activities were presented during the second RCM meeting (Vienna, March 16-20, 2015, Report IAEA INDC(NDS)-0682).

The new activities of ENEA were mainly focussed on the analysis of a *copper benchmark experiment* performed at FNG in 2015. The benchmark consisted in the irradiation with 14 MeV neutrons of a block of pure OFC copper (oxygen free) of 60x60x70 cm³. Several different measurements were carried out such as: *a)* reaction rate measurements in seven different penetration depths along the mid-plane of the block; *b)* neutron and gamma flux spectra measurements in two positions inside the Cu block; *c)* dose measurements in different positions inside the block by thermoluminescent dosimeters (TLD).

For the purposes of the present meeting, ENEA compared the reaction rates (RR) calculated inside the Cu block using IRDF-2002 and IRDFF-v1.05 dosimetry files. The nuclear responses were calculated with the MCNP5 code using JEFF-3.1.1/JEFF 3.2 and FENDL3 nuclear data library for transport. The activation reactions used were: $^{93}\text{Nb}(n,2n)^{92}\text{Nb}^m$, $^{197}\text{Au}(n,2n)^{196}\text{Au}$, $^{27}\text{Al}(n,a)^{24}\text{Na}$, $^{58}\text{Ni}(n,p)^{58}\text{Co}$, $^{115}\text{In}(n,n')^{115}\text{In}$, $^{186}\text{W}(n,\gamma)^{187}\text{W}$, $^{197}\text{Au}(n,\gamma)^{198}\text{Au}$, $^{55}\text{Mn}(n,\gamma)^{56}\text{Mn}$ which cover the whole neutron energy range for fusion neutronics.

The comparison between the RR calculated with IRDF-2002 and IRDFF_v1.05 addressed the following points :

- a) for all the used threshold reactions the results calculated using IRDF-2002 and IRDFF_v1.05 are almost the same within $\pm 1\div 2\%$ (Max.)
Larger discrepancies are observed for thermal sensors.
- b) $^{197}\text{Au}(n,\gamma)$: the IRDFF-v1.05 results *underestimate* the IRDF-2002 (v-2005) results by about 5-12 % (systematic increase with penetration depth)
- c) $^{186}\text{W}(n,\gamma)$ 20% (constant difference with penetration depth)
- d) $^{55}\text{Mn}(n,\gamma)$: the IRDFF_v1.05 results *overestimate* the IRDF-2002 results by about 10% (constant trend with penetration depth)

The causes of the observed discrepancies are under investigation, however it could be attributed to the observed differences in the thermal reaction cross section between the old IRDF-2002 and the new IRDFF_v1.05 files (e.g. see fig. 1). Differences in the centroid, width and high of the resonances have been observed for almost all the three used thermal sensors. A more deep analysis of the calculated RR has been performed by taking the ratio of the bin-to-bin calculated thermal RR (MCNP calculations were performed using the VITAMIN-J structure), an example is reported in fig. 2. The ratio clearly shows that in the resonance region the RR calculated by using IRDF-2002 and IRDFF_v1.05 can have not negligible differences. Again this is observed for all the three used thermal sensors.

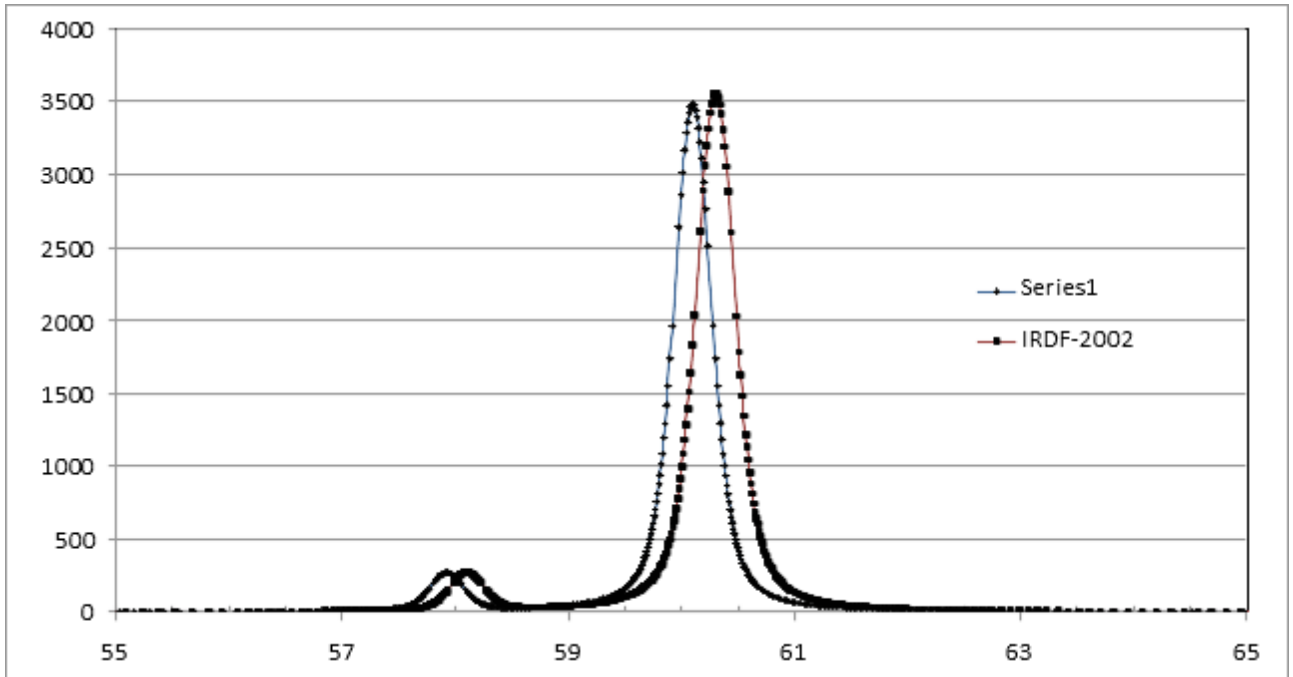


Fig. 1: $^{197}\text{Au}(n,g)$ cross section comparison between IRDFF_v1.05 and IRDF-2002 at around 60 eV

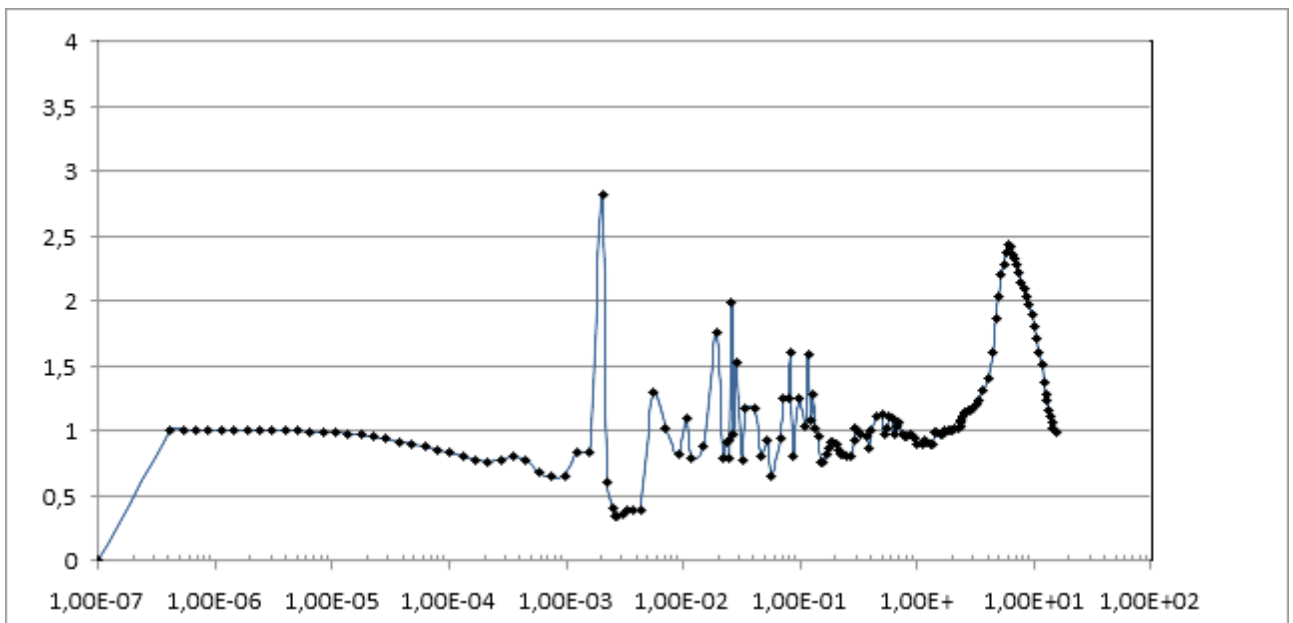


Fig. 2: R.R. ratio between calculation performed using IRDFF_v1.05 and IRDF-2002

As far as next activities are concerned, ENEA is proposing the participation to the REAL exercise. To this end, ENEA is proposing to use the experimental RR in some selected positions inside the Cu block to perform the spectra unfolding. The primary interest for ENEA is the comparison of the unfolded spectra in selected positions using different unfolding codes (e.g. SAND-II and STAYSL). ENEA will provide the neutron spectra in the VITAMIN-J structure obtained from MCNP5 calculations using FENDL and/or JEFF libraries.

Owing to the importance that copper has for the fusion plants, the comparison of other quantities derived from the unfolded neutron flux spectra can be also considered (e.g. dpa, doses etc.)

7.6. Final results of IRDFF benchmark test at JAEA/FNS, M. Ohta¹, S. Sato¹, S. Kwon¹, K. Ochiai¹, C. Konno²

¹ National Institutes for Quantum and Radiological Science and Technology, Rokkasyo-mura, Kamikita-gun, Aomori-ken, Japan

² Japan Atomic Energy Agency, Tokai-mura, Naka-gun, Ibaraki-ken, Japan

1. Introduction

At RCM1 we proposed the following items.

- 1) Comparison between IRDFF and cross section data around 14 MeV previously measured at JAEA/FNS.
- 2) Measurement of cross section data such as $^{nat}\text{Ti}(n,x)^{46}\text{Sc}$ around 14 MeV with natural foils.
- 3) Reaction rate measurement inside some experimental assemblies, neutron spectra in which are well specified in our benchmark experiments, such as graphite and Li_2O .

However we skipped the second item because the third item covers the second one. We reported our preliminary results with IRDFF v1.03 at RCM2, focusing on the reaction rate measurements inside the graphite and Li_2O assemblies. An additional experiment with the graphite assembly were carried out after RCM2 for some reactions, where half-lives of produced radio isotopes are shorter than ~ 40 min. However we could not perform a tungsten experiment to validate the $^{55}\text{Mn}(n,\gamma)$ and $^{58}\text{Fe}(n,\gamma)$ cross sections from 10 keV to 1 MeV, which were included in the action lists of RCM2, because of FNS shutdown in February, 2016. Here we present our results with IRDFF v1.05, most of which are almost the same as our presentation in RCM2.

2. Comparison between IRDFF and activation cross-section data measured previously at FNS

More than 20 years ago we measured activation cross-section data of more than 200 reactions around 14 MeV at FNS. IRDFF and our measured activation cross-section data for 38 threshold reactions in IRDFF v1.05 were compared from 13 to 15.25 MeV. The agreement between IRDFF and our measured activation cross-section data was good for the most reactions as shown in Fig. 1, though it was not so good for $^{29}\text{Si}(n,x)^{28}\text{Al}$, $^{48}\text{Ti}(n,x)^{47}\text{Sc}$, $^{64}\text{Zn}(n,p)^{64}\text{Cu}$ and $^{113}\text{In}(n,n')^{113m}\text{In}$ in which are shown in Fig. 2.

3. IRDFF benchmark experiments at FNS

A lot of nuclear data benchmark experiments have been carried out for 30 year at FNS. The graphite and Li_2O experiments showed much better agreement between measured and calculated data in the experiments. This means that the neutron characteristics are well specified with the calculation. The neutron spectra in the graphite and Li_2O assemblies are very different; that in the graphite assembly has not only DT neutrons but also low energy neutrons with thermal neutron peak, while that in the Li_2O assembly is very hard and has no thermal neutron peak, which is shown in Fig. 3. Thus we selected the graphite and Li_2O assemblies for benchmarking IRDFF.

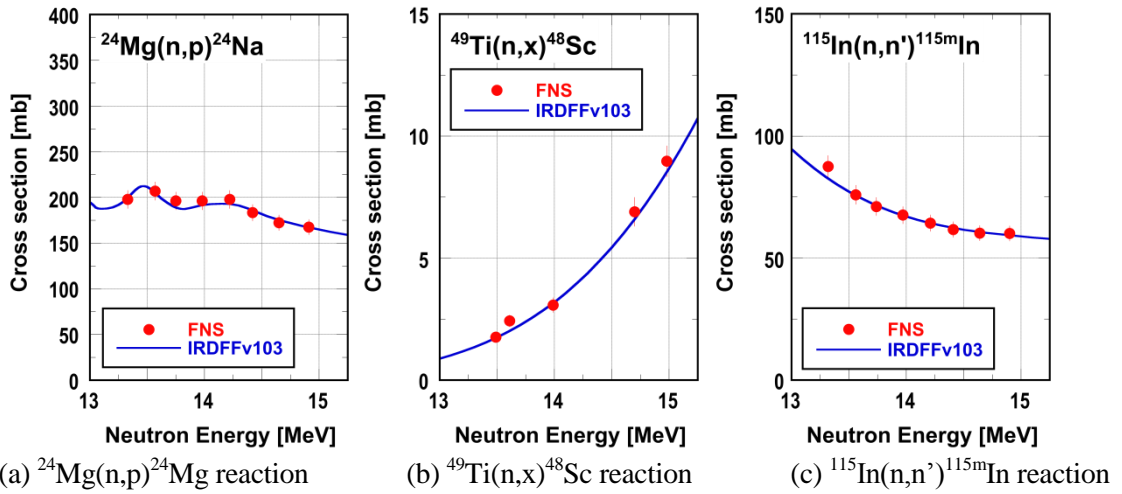


Fig. 1: Comparison of IRDFF and cross-section data measured at JAEA/FNS.

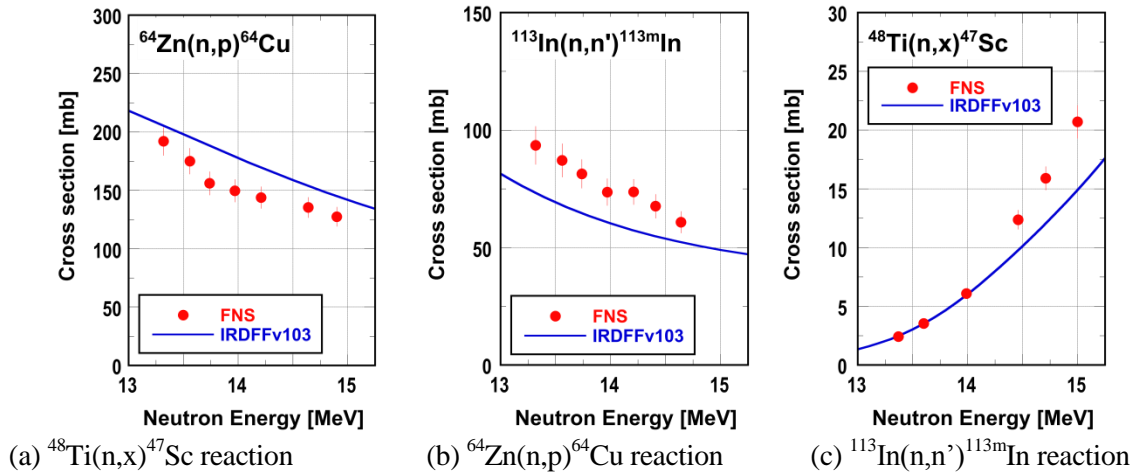


Fig. 2: Comparison of IRDFF and cross-section data measured at JAEA/FNS.

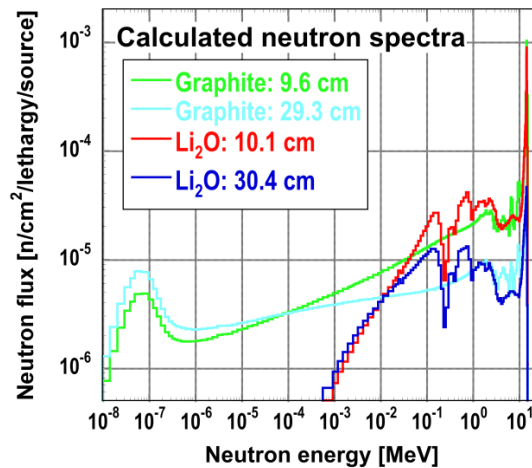


Fig. 3: Calculated neutron spectra at the measuring positions in graphite and Li₂O assemblies.

3.1. Graphite experiment with DT neutron source

We used the same graphite assembly as our previous graphite assembly; a pseudo-cylindrical graphite assembly of 63 cm in equivalent diameter and 61 cm in thickness as shown in Fig. 4. 28 foils were set at the depths of 9.6 and 29.3 cm in order to measure reaction rates of the reactions in IRDFF. The standard foils of Nb, In, and Au every ~ 10 cm were also set in order to check the neutron field in the graphite assembly. We irradiated the graphite assembly with DT neutron source of $\sim 1.5 \times 10^{11}$ n/sec for 5 hours twice in March 2014, because we had to set 28 foils at the same positions. Reaction rates of 40 reactions (half-lives of produced radio isotopes are longer than ~ 40 min.) in IRDFF v1.05 (79 reactions) were measured with Ge detectors. The experimental errors of the most measured reaction rates were less than 10%.

This experiment was analyzed by using a Monte Carlo neutron transport code MCNP5-1.40 with a nuclear data library ENDF/B-VII.1. The thermal scattering law data $S(\alpha, \beta)$ for graphite in ENDF/B-VII.1 was also used in the analysis. IRDFF-v1.05 was adopted as the cross section data for the reaction rate calculation. The reaction rates for the capture reactions with thicker foils were calculated by using the cell flux (F4) tally in order to correct neutron self-shielding. We did not carry out the error estimation for the calculated reaction rates with IRDFF covariance data yet. The measured reaction rates are compared with the calculated reaction rates in Fig. 4, which suggested if IRDFF data is good or not. Most of the 41 measured reaction rates agree with the calculated ones within 10%, while the measured reaction rates of the $^{181}\text{Ta}(n, \gamma)^{182}\text{Ta}$ and $^{204}\text{Pb}(n, n')^{204\text{m}}\text{Pb}$ did within 20%.

We also carried out an additional experiment with the graphite assembly in October, 2015, for 5 reactions, where half-lives of produced radio isotopes are shorter than ~ 40 min.; $^{27}\text{Al}(n, p)^{27}\text{Mg}$, $^{28}\text{Si}(n, p)^{28}\text{Al} + ^{29}\text{Si}(n, x)^{28}\text{Al}$, $^{54}\text{Fe}(n, 2n)^{53}\text{Fe}$, $^{63}\text{Cu}(n, 2n)^{62}\text{Cu}$. We irradiated the graphite assembly with DT neutron source of $\sim 1.5 \times 10^{11}$ n/sec for 10 min. five times, because the half-lives of the produced radio isotopes are short. Experimental error estimation and analysis method are similar with those in the previous graphite experiment. The 5 measured reaction rates agree with the calculated ones within 10% as shown in Fig. 5.

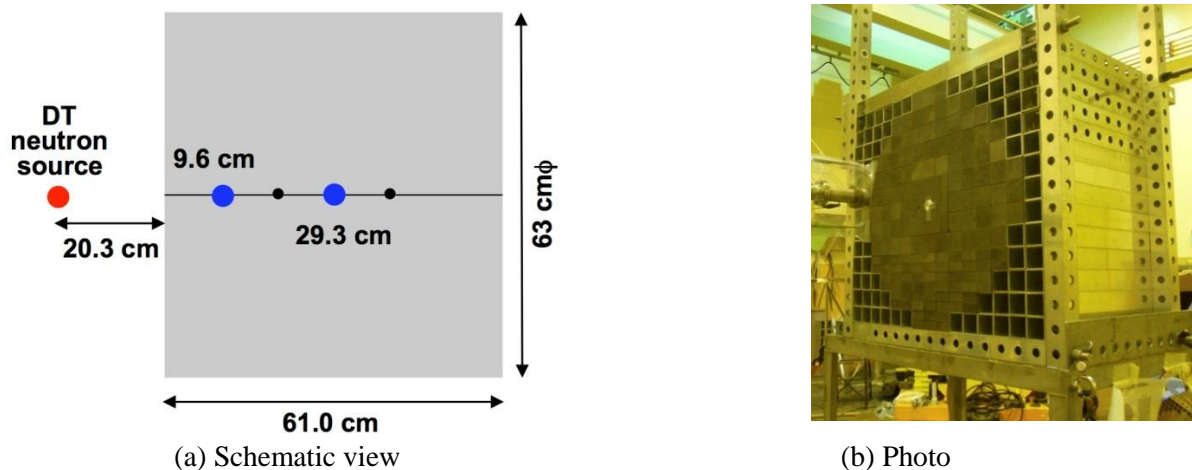


Fig. 4: Graphite assembly.

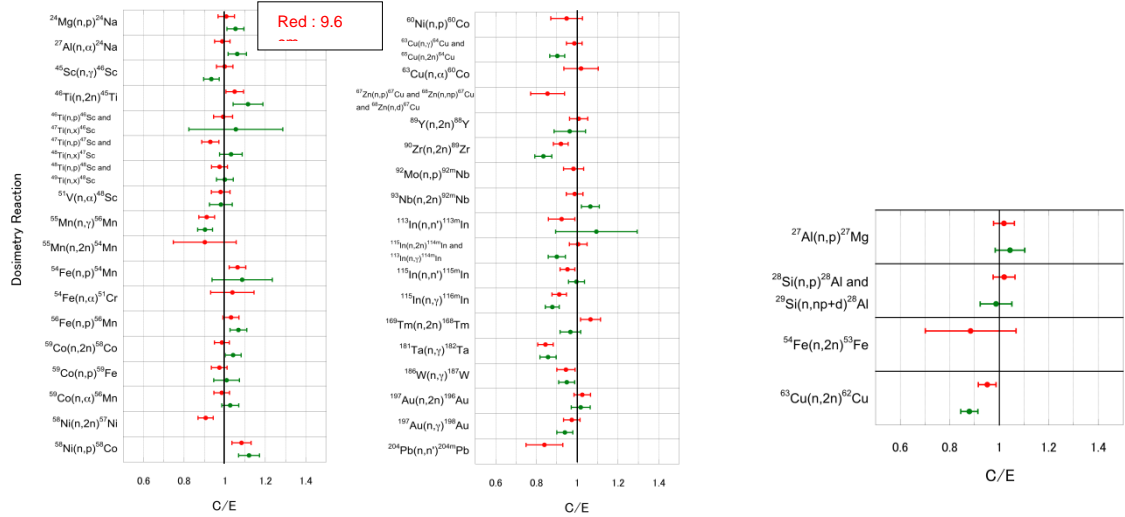


Fig. 5: Ratios of calculation to experiment (C/E) for reaction rates of reactions.

3.2. Li₂O experiment with DT neutron source

We used a rectangular Li₂O assembly of 65.7 cm in width, 65.7 cm in height and 60.7 cm in thickness as shown in Fig. 6. We carried out the similar experiment with the graphite one last November. Note that the neutron spectra are harder than those in the graphite experiment. Reaction rates of 31 reactions in IRDFF (79 reactions) were measured. Reaction rates of several reactions measured in the graphite experiment were not finalized yet. Experimental error estimation and analysis method are similar with those in the graphite experiment.

Most of the 30 measured reaction rates agreed with the calculated ones within 10%, while the measured reaction rates of the ⁴⁸Ti(n,p)⁴⁸Sc and ⁴⁹Ti(n,x)⁴⁸Sc, and ⁵¹V(n,α)⁴⁸Sc did within 20%, which is shown in Fig. 7.

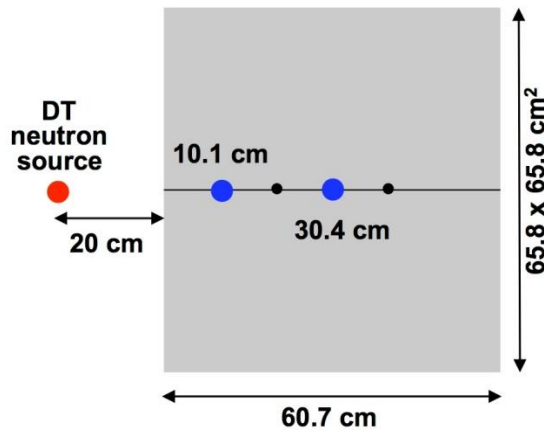


Fig. 6: Li₂O assembly.

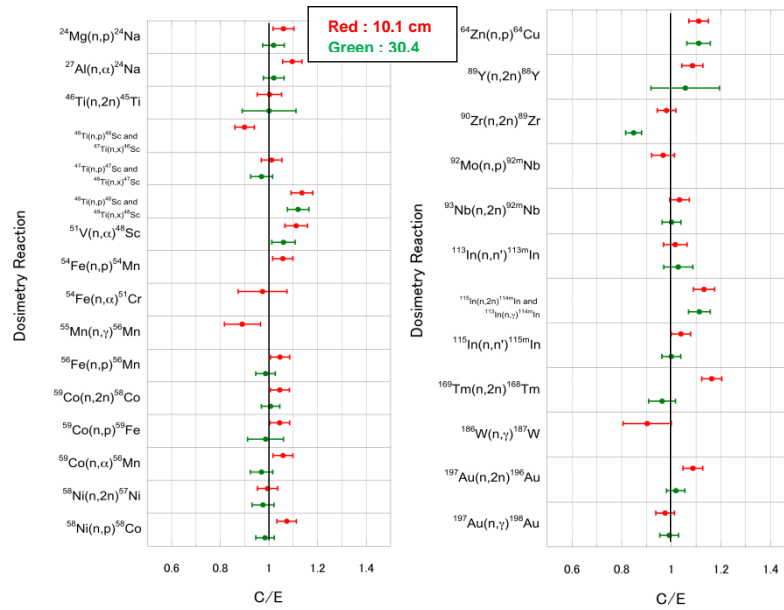


Fig. 7: Ratios of calculation to experiment (C/E) of reaction rates.

4. Summary

We have completed the following items for benchmarking IRDFF v1.05, though FNS shut down in February, 2016.

- Cross section comparison between IRDFF and our cross section data measured previously
- Graphite experiment with DT neutrons
- Li_2O experiment with DT neutrons.

It is confirmed that IRDFF is generally good. Additionally it is reported that the elastic cross section data should be added to ^{55}Mn , ^{58}Fe , ^{235}U and ^{238}U in IRDFF for self-shielding correction.

7.7. Improvements to STAYSL PNNL Spectral Adjustment with IRDFF, L.R. Greenwood and C.D. Johnson

Pacific Northwest National Laboratory, USA

Executive Summary

The STAYSL PNNL program [1] performs a least-squares adjustment of the neutron spectrum based on the IRDFF cross section library and user-defined activation data and a starting neutron spectrum. All known covariances are included. Required corrections are included for the irradiation history, gamma absorption, neutron burn-up, and neutron self-shielding using separate utility programs prior to the execution of STAYSL PNNL. Several new neutron cross section libraries based on IRDFF V1.05 to 60 MeV are provided with the program including energy group structures of 69 (WIMS), 129 (14 MeV), 140 (prior 100 groups extended to 60 MeV), 175 (Vitamin J), 640 (old SANDII to 20 MeV), and 725 (old Sand II extended to 60 MeV) energy groups. Five new reactions were included in IRDFF V1.05, namely SI28P, MN552, CO593, CO59P, ZN67P, MO92P, IN113N, IN113G, TM1693, BI2093, U235G, and U2382. Calculations are included to demonstrate the need for activation cross sections from natural targets such as $Ti(n,x)^{46}Sc$ rather than only isotopic targets such as $^{46}Ti(n,p)^{46}Sc$ and $^{47}Ti(n,x)^{46}Sc$. The effects of such reactions increase dramatically with increasing neutron energies and cannot be neglected. Some critical reactions such as $^{56}Fe(n,x)^{54}Mn$ are not currently included in IRDFF and prevent the use of the $^{54}Fe(n,p)^{54}Mn$ reaction at higher neutron energies. It is recommended that natural element cross sections be included in future releases of IRDFF for a list of reactions that suffer from reactions on multiple isotopes that lead to the same activation product. Spectral adjustments are illustrated in Be(d,n) thick target neutron fields at deuteron energies of 30 and 40 MeV.

Updates to Neutron Cross Section Libraries

Neutron cross section libraries provided with the STAYSL PNNL were updated with the latest release of IRDFF V1.05 to 60 MeV. Previously, the software only included one 100 group energy structure. Release 1.02 in August 2015 includes six nuclear data libraries in the following group structures:

- 69 groups (WIMS/EPRI-CPM)
- 129 groups (for 14 MeV neutron sources)
- 140 groups (prior 100 group structure extended to 60 MeV in 1 MeV bins)
- 175 groups (Vitamin J)
- 640 groups (SAND II to 20 MeV)
- 725 groups (SAND II extended to 60 MeV)

The 69, 129, and 640 group libraries do not include many reactions in IRDFF that have thresholds above the highest energy group in these specialized group structures. Neutron self-shielding calculations with the SHIELD module are performed in the correct group structure selected for all calculations by the user at run time.

Neutron cross sections were processed with the NJOY and NJPP programs. NJOY is not included with the program. Advanced users can create their own nuclear data libraries if they have access to NJOY or other software that can process the IRDFF cross section and covariance files distributed by the IAEA.

Five new reactions were included in IRDFF V1.05, SI28P, MN552, CO593, CO59P, ZN67P, MO92P, IN113N, IN113G, TM1693, BI2093, U235G, and U2382 where the short name such as MN552 refers to the $^{55}Mn(n,2n)^{54}Mn$ reaction.

The output of STAYSL PNNL was revised to list reaction rates in units of product atoms/target atoms – second to correspond to the input reaction rates rather than using barn units. The section called “Summary of Fluxes, Fluences, and Uncertainties” was revised to include the additional higher energy groups to 60 MeV. Users that created input files for the previous version of STAYSL PNNL only need to change the input number of groups to correspond to one of the new energy group structures (rather than the prior fixed value of 100 groups) and change the “mini group summary” that is provided for user convenience to include the new groups above 20 MeV as they see fit.

Problems with Contributions to Activation Products from Elements with Multiple Isotopes

All of the cross sections provided with IRDFF are listed on an isotopic basis, such as $^{46}\text{Ti}(n,p)^{46}\text{Sc}$. In practice, however, users of IRDFF almost always use natural elemental targets. With the increase in neutron energies to 60 MeV, there are many cases where specific activation products can be made from other isotopes of the same element, such as $^{47}\text{Ti}(n,x)^{46}\text{Sc}$. A review of the reactions included in IRDFF shows that many of the needed reactions are not present, as listed in Table 1. Unfortunately, many of the required reactions are not provided in IRDFF, thereby significantly limiting the utility of these reactions for any calculations or spectral adjustment at higher neutron energies. A very important example is $^{54}\text{Fe}(n,p)^{54}\text{Mn}$ which cannot be used at higher neutron energies since IRDFF does not include the larger production reaction of $^{56}\text{Fe}(n,x)^{54}\text{Mn}$, as discussed below. It is thus recommended that future releases of IRDFF include the missing reactions listed in Table 1. It would be most convenient for users of IRDFF if natural element cross sections be created such as $\text{Ti}(n,x)^{46}\text{Sc}$ by combining all of the isotopic reactions that contribute to the production of ^{46}Sc .

For fission reactor dosimetry, these effects are relatively small, as shown in Table 2, although the effects increase for fast reactors or if thermal neutrons are shielded by cadmium, for example. At higher neutron energies, it is critically important to include such reactions as shown by the calculations in Table 3 and the footnote.

Table 1: Summary of Reactions in IRDFF that Require Cross Sections from Other Isotopes

| Isotopic Reaction | Other Isotope Reactions | In IRDFF? | | Natural Reaction |
|--|---|-----------|-----|----------------------------------|
| $^{24}\text{Mg}(n,p)^{24}\text{Na}$ | $^{25}\text{Mg}(n,np+d)^{24}\text{Na}$ | No | | $\text{Mg}(n,x)^{24}\text{Na}$ |
| $^{28}\text{Si}(n,p)^{28}\text{Al}$ | $^{29}\text{Si}(n,np+d)^{28}\text{Al}$ | | Yes | $\text{Si}(n,x)^{28}\text{Al}$ |
| $^{46}\text{Ti}(n,p)^{46}\text{Sc}$ | $^{47}\text{Ti}(n,x)^{46}\text{Sc}$ | | Yes | $\text{Ti}(n,x)^{46}\text{Sc}$ |
| $^{47}\text{Ti}(n,p)^{47}\text{Sc}$ | $^{48}\text{Ti}(n,x)^{47}\text{Sc}$ | | Yes | $\text{Ti}(n,x)^{47}\text{Sc}$ |
| $^{48}\text{Ti}(n,p)^{48}\text{Sc}$ | $^{49}\text{Ti}(n,x)^{48}\text{Sc}$ | | Yes | $\text{Ti}(n,x)^{48}\text{Sc}$ |
| $^{52}\text{Cr}(n,2n)^{51}\text{Cr}$ | $^{50}\text{Cr}(n,\gamma)^{51}\text{Cr}$ | No | | $\text{Cr}(n,x)^{51}\text{Cr}$ |
| $^{54}\text{Fe}(n,p)^{54}\text{Mn}$ | $^{56}\text{Fe}(n,nd+t)^{54}\text{Mn}$ | No | | $\text{Fe}(n,x)^{54}\text{Mn}$ |
| $^{56}\text{Fe}(n,p)^{56}\text{Mn}$ | $^{57}\text{Fe}(n,np+d)^{56}\text{Mn}$ | No | | $\text{Fe}(n,x)^{56}\text{Mn}$ |
| $^{58}\text{Ni}(n,2n)^{57}\text{Ni}$ | $^{60}\text{Ni}(n,4n)^{57}\text{Ni}$; etc. | No | | $\text{Ni}(n,xn)^{57}\text{Ni}$ |
| $^{58}\text{Ni}(n,p)^{58}\text{Co}$ | $^{60}\text{Ni}(n,x)^{58}\text{Co}$ | No | | $\text{Ni}(n,x)^{58}\text{Co}$ |
| $^{63}\text{Cu}(n,g)^{64}\text{Cu}$ | $^{65}\text{Cu}(n,2n)^{64}\text{Cu}$ | | Yes | $\text{Cu}(n,x)^{64}\text{Cu}$ |
| $^{64}\text{Zn}(n,p)^{64}\text{Cu}$ | $^{66}\text{Zn}(n,x)^{64}\text{Cu}$ | No | | $\text{Zn}(n,x)^{64}\text{Cu}$ |
| $^{67}\text{Zn}(n,p)^{67}\text{Cu}$ | $^{68}\text{Zn}(n,x)^{67}\text{Cu}$ | No | | $\text{Zn}(n,x)^{67}\text{Cu}$ |
| $^{90}\text{Zr}(n,2n)^{89}\text{Zr}$ | $^{91}\text{Zr}(n,3n)^{89}\text{Zr}$; etc. | No | | $\text{Zr}(n,xn)^{89}\text{Zr}$ |
| $^{92}\text{Mo}(n,p)^{92m}\text{Nb}$ | $^{94}\text{Mo}(n,x)^{92m}\text{Nb}$ | No | | $\text{Mo}(n,x)^{92m}\text{Nb}$ |
| $^{113}\text{In}(n,g)^{114m}\text{In}$ | $^{115}\text{In}(n,2n)^{114m}\text{In}$ | | Yes | $\text{In}(n,x)^{114m}\text{In}$ |

Table 2: Calculation of Isotopic Effects for Thermal Fission Reactors

| Reaction | SigPhi, At/at-s | Reaction | SigPhi, At/at-s | Isotopic Abundance | Activity Increase |
|------------------|-----------------|-------------------|-----------------|--------------------|-------------------|
| Tl46(N,P)SC46 | 7.1360E-12 | Tl47(N,X)SC46 | 3.3338E-14 | 8.25/ 7.44 | 0.42 % |
| Tl47(N,P)SC47 | 1.2223E-11 | Tl48(N,X)SC47 | 9.7335E-15 | 7.44/ 73.72 | 0.79 % |
| Tl48(N,P)SC48 | 2.2220E-13 | Tl49(N,X)SC48 | 5.9619E-15 | 73.72/ 5.41 | 0.20 % |
| CU63(N,G)CU64* | 6.0667E-09 | CU65(N,2N)CU64 | 5.9619E-13 | 69.15/ 30.85 | 0.0044 % |
| IN113(N,G)IN114M | 3.2563E-08 | IN115(N,2N)IN114M | 1.2127E-12 | 4.29/ 95.71 | 0.083 % |

*Values are for the PTP position in the High Flux Isotope Reactor at ORNL

Table 3: Calculation of Isotopic Effects for Be(d,n) Neutron Field at $E_d = 30$ MeV [2]. See Figures 1 and 2 for the neutron spectra used for these calculations

| Reaction | SigPhi, At/at-s | Reaction | SigPhi, At/at-s | Isotopic Abundance | Activity Increase |
|-------------------|-----------------|------------------|-----------------|--------------------|-------------------|
| Tl46(N,P)SC46 | 1.5363E-13 | Tl47(N,X)SC46 | 4.9729E-14 | 8.25/ 7.44 | 29% |
| Tl47(N,P)SC47 | 8.6925E-14 | Tl48(N,X)SC47 | 2.3424E-14 | 7.44/ 73.72 | 367% |
| Tl48(N,P)SC48 | 2.7493E-14 | Tl49(N,X)SC48 | 1.4607E-14 | 73.72/ 5.41 | 3.9% |
| CU65(N,2N)CU64 | 3.7463E-13 | CU63(N,G)CU64 | 7.3686E-15* | 30.85/ 69.15 | 4.4%* |
| IN115(N,2N)IN114M | 5.6409E-13 | IN113(N,G)IN114M | 8.0340E-14 | 95.71/ 4.29 | 0.63%* |

*At $E_d = 40$ MeV, the activity increases are 69% (^{46}Sc), 790% (^{47}Sc), and 9.4% (^{48}Sc). Thermal reaction calculations have a high uncertainty since the thermal region is below the range of the neutron time-of-flight data.

As shown in Table 3, it becomes critical to include contributions from higher isotopes or competing reactions at higher neutron energies. Spectral adjustments for Be(d,n) neutron sources are shown in Figures 1 and 2 with the corresponding comparison of measured and calculated reaction rates in Tables 4 and 5. As can be seen, there are significant discrepancies for the $^{54}\text{Fe}(n,p)^{54}\text{Mn}$ reaction due to the failure to take into account the missing contributions from the $^{56}\text{Fe}(n,x)^{54}\text{Mn}$ reaction. Consequently, the $^{54}\text{Fe}(n,p)^{54}\text{Mn}$ reaction in IRDF cannot be reliably used for spectral adjustment at higher neutron energies. Similarly, many of the other missing reactions listed in Table 1 lead to the same conclusion for these reactions.

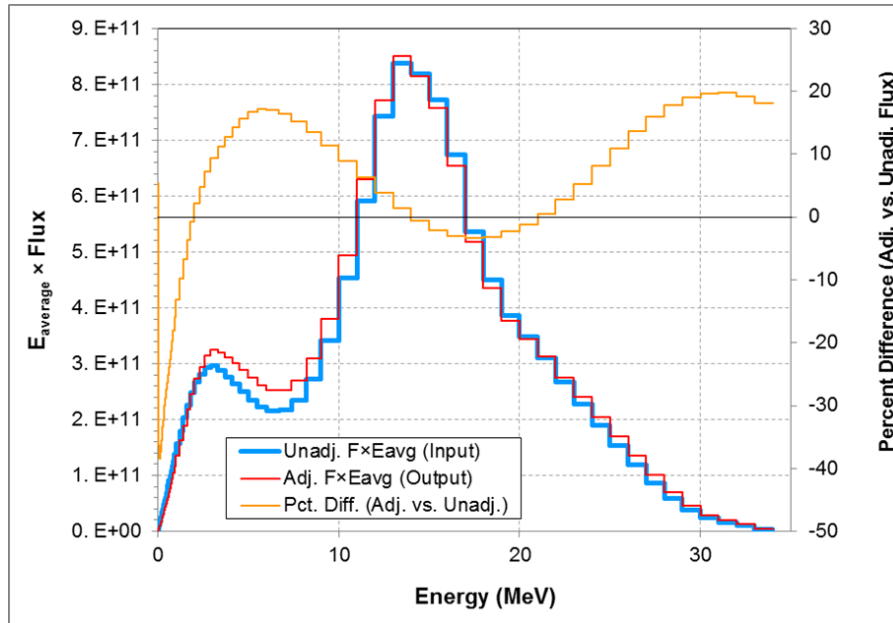


Fig. 1: Be(d,n) spectral adjustment at $E_d = 30$ MeV (reference 2)

Table 4: STAYSL PNNL spectral adjustment output for Be(d,n) source at $E_d=30$ MeV

| INPUT NORMALIZATION DATA | | | | | | | | | | | |
|--------------------------|-----------|----------|------------------------|--------|-------------------|--------|------------------|----------------------|-----------|-------------------|------------|
| AK1 | = | 1.00000 | VAK | = | 0.00090 | | | | | | |
| NORML | = | 0 | RENORM | = | 1.00000 | | | | | | |
| CHI ² | = | 18.74312 | NORM. CHI ² | = | 1.44178 | | | | | | |
| DOSIMETRY ACTIVITIES | | | | | | | | | | | |
| RXN | INPUTS | | -UNADJUSTED FLUX- | | - ADJUSTED FLUX - | | CHI ² | 90% ACTIVITIES RANGE | | REACTION | |
| | MEASURED | ±% | ACTIVITY | %DIFF | ACTIVITY | %DIFF | | CONTRIB | --LOW E-- | | --HIGH E-- |
| 1 | 3.850E+10 | 3.00 | 4.855E+10 | 26.10 | 3.906E+10 | 1.46 | 3.984 | 4.50E-05 | 3.70E+00 | AU197 (N,G)AU198 | |
| 2 | 3.960E+09 | 3.00 | 4.416E+09 | 11.51 | 3.934E+09 | -0.66 | -0.381 | 1.00E-04 | 1.30E+01 | CO59 (N,G)CO60 | |
| 3 | 3.570E+11 | 10.00 | 2.795E+11 | -21.72 | 3.017E+11 | -15.50 | 3.277 | 3.30E+00 | 1.60E+01 | FE54 (N,P)MN54 | |
| 4 | 3.710E+11 | 3.00 | 3.307E+11 | -10.85 | 3.584E+11 | -3.40 | 3.512 | 2.90E+00 | 1.60E+01 | NI58 (N,P)CO58 | |
| 5 | 7.750E+10 | 10.00 | 6.538E+10 | -15.64 | 6.797E+10 | -12.29 | 1.897 | 7.40E+00 | 1.90E+01 | NI60 (N,P)CO60 | |
| 6 | 2.830E+10 | 7.00 | 2.673E+10 | -5.55 | 2.781E+10 | -1.74 | 0.179 | 6.00E+00 | 2.10E+01 | CO59 (N,P)FE59 | |
| 7 | 1.800E+10 | 10.00 | 1.882E+10 | 4.54 | 1.886E+10 | 4.76 | 0.210 | 1.40E+01 | 2.60E+01 | NI58 (N,2N)NI57 | |
| 8 | 2.950E+11 | 3.00 | 2.939E+11 | -0.36 | 2.934E+11 | -0.55 | 0.018 | 1.20E+01 | 2.30E+01 | CO59 (N,2N)CO58 | |
| 9 | 9.110E+09 | 5.00 | 7.764E+09 | -14.78 | 8.582E+09 | -5.79 | 1.791 | 2.10E+01 | 3.00E+01 | CO59 (N,3N)CO57 | |
| 10 | 8.880E+11 | 3.00 | 8.818E+11 | -0.70 | 8.938E+11 | 0.65 | -0.051 | 1.00E+01 | 2.00E+01 | AU197 (N,2N)AU196 | |
| 11 | 3.360E+11 | 3.00 | 3.339E+11 | -0.63 | 3.328E+11 | -0.94 | 0.049 | 1.30E+01 | 2.40E+01 | ZR90 (N,2N)ZR89 | |
| 12 | 1.830E+11 | 3.00 | 1.918E+11 | 4.83 | 1.936E+11 | 5.81 | 3.119 | 1.00E+01 | 2.00E+01 | NB93 (N,2N)NB92M | |
| 13 | 5.410E+10 | 3.00 | 5.148E+10 | -4.84 | 5.302E+10 | -2.00 | 1.052 | 8.20E+00 | 1.80E+01 | AL27 (N,A)NA24 | |
| 14 | 4.380E+10 | 20.00 | 4.060E+10 | -7.30 | 4.160E+10 | -5.03 | 0.087 | 7.40E+00 | 2.00E+01 | FE54 (N,A)CR51 | |
| ± STD. DEV. = | | | 12.46 | | 6.38 | | | | | | |

The STAYSL PNNL spectral adjustment output in Figures 1 and 2 and Tables 4 and 5 show excellent agreement between most of the measured and calculated reaction rates at energies up to 30 MeV. In these cases, the neutron spectra are quite well known since they were measured by neutron time-of flight. These adjustments are considered preliminary since the full covariance matrix for the neutron spectra are still under development.

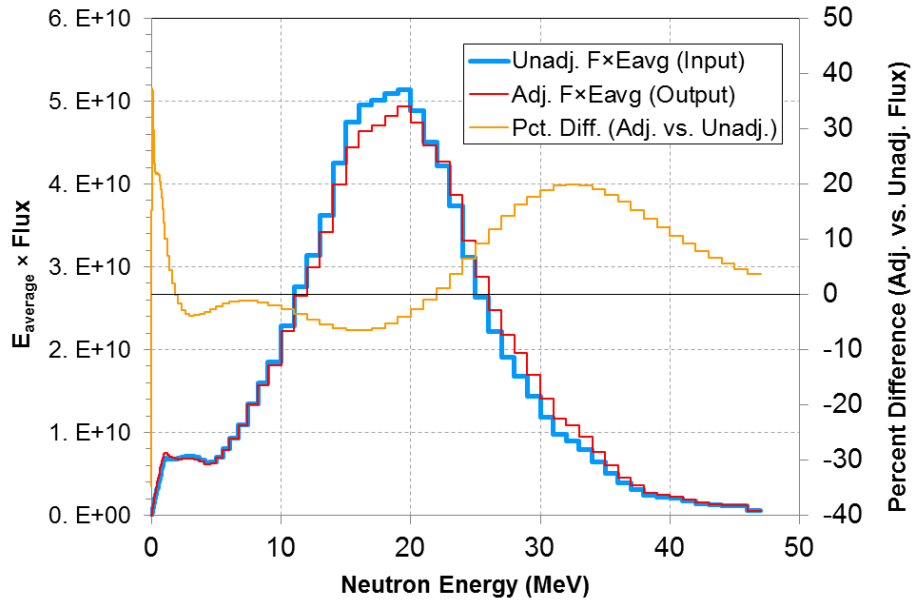


Fig. 2: Be(d,n) spectral adjustment at $E_d = 40$ MeV [3, 4]

Table 5: STAYSL PNNL spectral adjustment output for Be(d,n) source at $E_d=40$ MeV

| INPUT NORMALIZATION DATA | | | | | | | | | | | | | |
|--------------------------|-----------|----------|------------------------|-----------|-----------------|-------|---------------|--------|------------------|----------|----------------------|---------------------|--|
| AK1 | = | 0.01700 | VAK | = | 0.00090 | | | | | | | | |
| NORML | = | 0 | RENORM | = | 1.70000E-02 | | | | | | | | |
| CHI ² | = | 41.32954 | NORM. CHI ² | = | 1.96807 | | | | | | | | |
| DOSIMETRY ACTIVITIES | | | | | | | | | | | | | |
| RXN | MEASURED | ±% | INPUTS | ACTIVITY | UNADJUSTED FLUX | %DIFF | ADJUSTED FLUX | %DIFF | CHI ² | CONTRIB | 90% ACTIVITIES RANGE | REACTION | |
| | | | | | | | | | | | --LOW E-- | --HIGH E-- | |
| 1 | 2.500E-15 | 3.00 | | 2.274E-15 | -9.05 | | 2.574E-15 | 2.96 | -2.816 | 3.60E-04 | 2.30E+00 | AU197 (N,G) AU198 | |
| 2 | 3.380E-16 | 20.00 | | 2.144E-16 | -36.56 | | 2.383E-16 | -29.50 | 2.677 | 1.00E-04 | 1.30E+01 | CO59 (N,G) CO60 | |
| 3 | 2.130E-16 | 3.00 | | 1.810E-16 | -15.00 | | 2.088E-16 | -1.95 | 0.388 | 5.50E-03 | 1.50E+01 | SC45 (N,G) SC46 | |
| 4 | 7.820E-15 | 3.00 | | 8.530E-15 | 9.07 | | 8.393E-15 | 7.33 | 4.946 | 1.40E+00 | 2.20E+01 | IN115 (N,N') IN115M | |
| 5 | 3.800E-15 | 5.00 | | 2.897E-15 | -23.77 | | 3.291E-15 | -13.40 | 11.444 | 9.20E-03 | 2.60E+00 | IN115 (N,G) IN116M | |
| 6 | 4.830E-14 | 3.00 | | 5.475E-14 | 13.35 | | 5.251E-14 | 8.71 | 9.182 | 1.00E+01 | 2.30E+01 | TM169 (N,2N) TM168 | |
| 7 | 2.790E-14 | 3.00 | | 2.522E-14 | -9.62 | | 2.595E-14 | -6.98 | 2.582 | 1.80E+01 | 3.00E+01 | TM169 (N,3N) TM167 | |
| 8 | 3.050E-15 | 3.00 | | 3.188E-15 | 4.52 | | 3.088E-15 | 1.23 | 0.311 | 8.20E+00 | 2.50E+01 | FE56 (N,P) MN56 | |
| 9 | 1.640E-14 | 3.00 | | 1.580E-14 | -3.69 | | 1.532E-14 | -6.57 | 2.052 | 3.70E+00 | 2.00E+01 | NI58 (N,P) CO58 | |
| 10 | 3.980E-15 | 10.00 | | 3.835E-15 | -3.65 | | 3.701E-15 | -7.02 | 0.240 | 7.40E+00 | 2.40E+01 | NI60 (N,P) CO60 | |
| 11 | 1.600E-15 | 7.00 | | 1.739E-15 | 8.71 | | 1.692E-15 | 5.78 | 0.893 | 7.40E+00 | 2.60E+01 | CO59 (N,P) FE59 | |
| 12 | 1.880E-15 | 10.00 | | 2.134E-15 | 13.51 | | 2.133E-15 | 13.44 | 1.698 | 1.40E+01 | 2.90E+01 | NI58 (N,2N) NI57 | |
| 13 | 2.470E-14 | 3.00 | | 2.480E-14 | 0.42 | | 2.409E-14 | -2.46 | -0.077 | 1.20E+01 | 2.60E+01 | CO59 (N,2N) CO58 | |
| 14 | 2.570E-15 | 15.00 | | 2.009E-15 | -21.84 | | 2.254E-15 | -12.28 | 1.121 | 2.20E+01 | 3.60E+01 | CO59 (N,3N) CO57 | |
| 15 | 7.790E-16 | 3.00 | | 7.981E-16 | 2.45 | | 7.663E-16 | -1.64 | -0.144 | 9.00E+00 | 2.30E+01 | CO59 (N,A) MN56 | |
| 16 | 5.490E-14 | 3.00 | | 5.785E-14 | 5.37 | | 5.548E-14 | 1.06 | 0.629 | 1.00E+01 | 2.30E+01 | AU197 (N,2N) AU196 | |
| 17 | 3.270E-14 | 3.00 | | 3.350E-14 | 2.44 | | 3.298E-14 | 0.85 | 0.148 | 1.40E+01 | 2.70E+01 | ZR90 (N,2N) ZR89 | |
| 18 | 1.240E-14 | 3.00 | | 1.319E-14 | 6.38 | | 1.266E-14 | 2.10 | 1.498 | 1.10E+01 | 2.30E+01 | NB93 (N,2N) NB92M | |
| 19 | 3.140E-15 | 3.00 | | 3.053E-15 | -2.78 | | 2.924E-15 | -6.87 | 2.101 | 8.20E+00 | 2.10E+01 | AL27 (N,A) NA24 | |
| 20 | 3.960E-15 | 20.00 | | 2.692E-15 | -32.03 | | 2.592E-15 | -34.54 | 2.442 | 8.20E+00 | 2.40E+01 | FE54 (N,A) CR51 | |
| 21 | 1.220E-13 | 3.00 | | 1.210E-13 | -0.79 | | 1.221E-13 | 0.08 | -0.016 | 3.60E-01 | 2.90E+01 | U235 (N, FISSION) | |
| 22 | 6.800E-14 | 3.00 | | 6.777E-14 | -0.34 | | 6.738E-14 | -0.91 | 0.030 | 3.30E+00 | 3.00E+01 | U238 (N, FISSION) | |
| % | | | | STD. DEV. | = | 14.57 | | 11.86 | | | | | |

Table 6: Calculation of Isotopic Contributions for Reactions at Be(d,n), $E_d = 40$ MeV

| Reaction | Measured | Calculated * | M/C | Comment |
|---------------|----------|------------------|------|---------------------------------|
| FE54(N,P)MN54 | 2.87E-14 | 1.35E-14 | 2.12 | FE56(N,X)MN54 effect unknown |
| TI46(N,P)SC46 | 1.72E-14 | 8.18E-15 x 1.69 | 1.24 | TI47(N,X)SC46 addition too low? |
| TI47(N,P)SC47 | 4.01E-14 | 4.51E-15 x 8.90 | 1.00 | TI48(N,X)SC47 addition correct |
| TI48(N,P)SC48 | 1.83E-15 | 1.80E-15 x 1.094 | 0.93 | TI49(N,X)SC48 addition small |

* Thermal reactions not included since the thermal flux is below the range of the neutron time-of-flight measurements.

Table 6 shows a calculation of isotopic effects for the Be(d,n) neutron spectrum at $E_d = 40$ MeV, as shown in Figure 2 and Table 5. In this case, the measured ^{54}Mn activation rate is more than a factor of two higher than predicted by the $^{54}\text{Fe}(n,p)^{54}\text{Mn}$ reaction since we are not including the activation from the $^{56}\text{Fe}(n,x)^{54}\text{Mn}$ reaction (which is not included in IRDFF). For the three titanium reactions, calculations show that including the contributions from the other isotopes included in IRDFF give good agreement for ^{47}Sc and ^{48}Sc , but appear to be too low for ^{46}Sc , most likely suggesting that the $^{47}\text{Ti}(n,x)^{46}\text{Sc}$ reaction cross section may be too low at higher neutron energies.

Conclusions and Future Work

We recommend that future releases of IRDFF include the missing reactions listed in Table 1. Without these missing reactions, it may not be possible to use many of the IRDFF cross sections at higher neutron energies. For convenience of the user, it is most useful to provide cross sections from natural elements that add up all of the isotopic reactions leading to a specific activation product. We will update the STAYSL PNNL program with any future releases of IRDFF.

We are working on a future release of STAYSL PNNL that will switch the roles of the neutron cross sections and neutron spectra so that cross sections can be adjusted. This will be very useful in cases where measurements have been made in neutron spectra that are standards or have been characterized by the time-of-flight technique. Work is needed on defining the covariances of such spectra. The covariances are also required for a future REAL exercise to compare the results from various neutron codes used for spectral adjustment.

References

- [1] LR Greenwood and CD Johnson, "Least-Squares Spectral Adjustment with STAYSL PNNL," 15th International Symposium on Reactor Dosimetry, 18-23 May 2014, Aix-en-Provence, France, EPJ Web of Conferences, Vol. 106, 586-593, 2016 DOI:10.1051/epjconf/201610607001
- [2] D. W. Kneff et al., Symposium on Neutron Cross Sections from 10 to 50 MeV, BNL-NCS-51245, pp. 113-132, May 1980.
- [3] Greenwood, L. R., *et al.*, Nucl. Sci. Eng. **72** (1979) 175-190.
- [4] Saltmarsh, M. J., *et al.*, Nucl. Instrum. Methods **145** (1977) 81-90.

3-rd RCM of the CRP on
***"Testing and Improving the IAEA International Dosimetry
 Library for Fission and Fusion (IRDF)*"**

IAEA Headquarters, Vienna, Austria
 20-24 March 2017
 Meeting Room VIC C0440/C0437

Preliminary AGENDA

Monday, 20 March

09:00 - 09:30 **Registration** (IAEA Registration desk, Gate 1)

09:30 - 10:15 **Opening Session**

Welcoming address and Introduction – *A. Koning*

Introduction – *A. Trkov*

Election of Chairman and Rapporteur

Adoption of Agenda

Administrative matters

10:15 - 12:30 **General (about 45 min each)**

1. S. Simakov "Some outcomes from the IAEA CRP F41031 on Testing and Improving the International Reactor Dosimetry and Fusion File (IRDF)"
2. M. Kostal: "Correct implementation of the analysis schemes to use experiments for use as benchmarks for nuclear data validation"

12:30 – 14:00 **Lunch**

14:00 – 17:30 **Experimental measurements**

3. H. Yashima: "Activation cross section measurements for Bi and Co by 80 and 140 MeV p-Li quasi-monoenergetic neutrons"
4. Simeckova

Tuesday, 21 March

09:00 - 12:30 **Experimental measurements and analysis**

5. N.B. Ndlovu: "Cross-section measurements for neutron-induced reactions in Co, Au, Bi and Tm at neutron energies of 90 MeV and 140 MeV"
6. C. Destouches "Overview of recent integral cross section measurements and nuclear data performed at CEA reactor facilities"
7. Open

12:30 – 14:00 **Lunch**

14:00 – 17:30 **Mesurements and evaluations**

8. V. Chechev: "Analyzing and updating nuclear decay data evaluations to improve the IRDF Decay sub-library"
9. K. Zolotarev: "Evaluation of $^{23}\text{Na}(n,\gamma)^{24}\text{Na}$, $^{23}\text{Na}(n,2n)^{22}\text{Na}$, and $^{27}\text{Al}(n,2n)^{26}\text{Al}$ reaction cross sections for the IRDF library"

Wednesday, 22 March

09:00 - 12:30 Benchmarking and validation

10. P. Griffin: “Advanced UQ Approaches to the Validation of Dosimetry Cross Sections in Reactor Benchmark Fields”
11. M. Angelone: "Benchmarking of IRDFF Against 14 MeV Neutron Experiments“
12. C. Konno: “Final results of IRDFF benchmark experiments at JAEA/FNS”

12:30 – 14:00 Lunch

14:00 – 17:30 Benchmarking and validation

13. L. Greenwood: “Improvements to STAYSL PNNL Spectral Adjustment with IRDFF”
14. I. Kodeli: “Proposals for REAL-201X Spectra Adjustment Exercise: TRIGA and ASPIS-IRON88 measurements for IRDFF validation”

Thursday, 23 March

09:00 - 12:30 Round Table Discussion

Discussions on the fulfilment of objectives

12:30 – 14:00 Lunch

14:00 – 17:30 Round table discussion (cont'd)

Drafting of the Summary Report and Action List for Final Report

Friday, 24 March

09:00 - 14:00 Drafting of the summary report

Finalisation of the Summary Report and Action List

14:00 Closing of the meeting



**Third Research Coordination Meeting on
Testing and Improving the IAEA International Reactor
Dosimetry and Fusion File (IRDF)**

**20 – 24 March 2017
Room C 0440, Vienna, Austria**

LIST OF PARTICIPANTS

| | |
|--|--|
| <p>CZECH REPUBLIC Mr Michal KOSTAL Nuclear Physics Institute Hlavni 130 Rez 25068 E-mail: michal.kostal@evrez.cz</p> | <p>CZECH REPUBLIC Ms Eva SIMECKOVA Nuclear Physics Institute Hlavni 130 Rez 25068 E-mail: simeckova@ujf.cas.cz</p> |
| <p>FRANCE Mr Christophe DESTOUCHES CEA – Centre d'études nucléaires de Cadarache DER , B.P. 1 13108 St. Paul Lez Durance E-mail: christophe.destouches@cea.fr</p> | <p>GERMANY Mr Stanislav SIMAKOV Institute for Neutron Physics and Reactor Technology Karlsruhe Institute for Technology (KIT) Hermann-von-Heimholtz Platz 1 Eggenstein-Leopoldshafen 76344 E-mail: smkv@gmx.de</p> |
| <p>ITALY Mr Maurizio ANGELONE Division of Fusion Centro Ricerche Energia Via Enrico Fermi 27 Frascati 00044 E-mail: maurizio.angelone@enea.it</p> | <p>JAPAN Mr Chikara KONNO Japan Atomic energy Agency Tokai-mura, Naka-gun Ibaraki-ken 319-1195 E-mail: konno.chikara@jaea.go.jp</p> |

| | |
|--|--|
| <p>JAPAN Mr Hiroshi YASHIMA Kyoto University Research Reactor Institute Kumatori-cho, Sennan-gun Osaka 590-0494 E-mail: yashima@rri.kyoto-u.ac.jp</p> | <p>RUSSIAN FEDERATION Mr Valery CHECHEV Khlopin Radium Institute 2 Murinsky prospekt 28 194021 St. Petersburg E-mail: chechev@khlopin.ru</p> |
| <p>RUSSIAN FEDERATION Mr Konstantin ZOLOTAREV Institute for Physics and Power Engineering Bondarenko Sq. 1 249033 Obninsk E-mail: zki1946@mail.ru</p> | <p>SLOVENIA Mr Ivan Aleksander KODELI Jozef Stefan Institute Jamova cesta39 1000 Ljubljana E-mail: ivan.kodeli@ijs.si</p> |
| <p>SOUTH AFRICA Ms N.B. (Zina) NDLOVU iThemba Laboratory for Accelerator-based Sc. Old Faure Road, Faure 7131, P.O. Box 722 7129 Somerset West E-mail: nbndlovu@tlabs.ac.za</p> | <p>UNITED STATES OF AMERICA Mr Lawrence GREENWOOD Pacific Northwest Laboratory 902 Battelle Boulevard, P.O. box 999 Richland, WA 99352 E-mail: larry.greenwood@pnl.gov</p> |
| <p>UNITED STATES OF AMERICA Mr Patrick GRIFFIN Sandia National Laboratory P.O. Box 5820 Albuquerque NM 87185 E-mail: pjgriff@sandia.gov</p> | |
| <p>IAEA Mr Andrej TRKOV (Scientific Secretary) Nuclear Data Development Unit Nuclear Data Section Division of Physical and Chemical Sciences Tel.: +1 2600 21712 E-mail: A.Trkov@iaea.org</p> | <p>IAEA Mr Arjan KONING Head, Nuclear Data Section Division of Physical and Chemical Sciences Tel.: +1 2600 21709 E-mail: A.Koning@iaea.org</p> |
| <p>IAEA Mr Roberto CAPOTE NOY Head, Nuclear Data Development Unit Nuclear Data Section Division of Physical and Chemical Sciences Tel.: +1 2600 21713 E-mail: r.capotenoy@iaea.org</p> | <p>IAEA Mr Naohiko OTSUKA Nuclear Data Services Unit Nuclear Data Section Division of Physical and Chemical Sciences Tel.: +1 2600 21715 E-mail: N.Otsuka@iaea.org</p> |
| <p>IAEA Ms Valentina Semkova Nuclear Data Services Unit Nuclear Data Section Division of Physical and Chemical Sciences Tel.: +1 2600 21727 E-mail: V.Semkova@iaea.org</p> | |

Nuclear Data Section
International Atomic Energy Agency
Vienna International Centre, P.O. Box 100
A-1400 Vienna, Austria

E-mail: nds.contact-point@iaea.org
Fax: (43-1) 26007
Telephone: (43-1) 2600 21725
Web: <http://www-nds.iaea.org>
